Molecular Biology of the Cell
Vol. 8, 367–385, February 1997

Evidence for Physical and Functional Interactions among Two *Saccharomyces cerevisiae* SH3 Domain Proteins, an Adenylyl Cyclase-associated Protein and the Actin Cytoskeleton

Thomas Lila and David G. Drubin*

Department of Molecular and Cell Biology, University of California, Berkeley, California 94720

Submitted July 5, 1996; Accepted November 18, 1996
Monitoring Editor: David Botstein

In a variety of organisms, a number of proteins associated with the cortical actin cytoskeleton contain SH3 domains, suggesting that these domains may provide the physical basis for functional interactions among structural and regulatory proteins in the actin cytoskeleton. We present evidence that SH3 domains mediate at least two independent functions of the *Saccharomyces cerevisiae* actin-binding protein Abp1p in vivo. Abp1p contains a single SH3 domain that has recently been shown to bind in vitro to the adenylyl cyclase-associated protein Srv2p. Immunofluorescence analysis of Srv2p subcellular localization in strains carrying mutations in either *ABP1* or *SRV2* reveals that the Abp1p SH3 domain mediates the normal association of Srv2p with the cortical actin cytoskeleton. We also show that a site in Abp1p itself is specifically bound by the SH3 domain of the actin-associated protein Rvs167p. Genetic analysis provides evidence that Abp1p and Rvs167p have functions that are closely interrelated. *Abp1* null mutations, like *rvs167* mutations, result in defects in sporulation and reduced viability under certain suboptimal growth conditions. In addition, mutations in *ABP1* and *RVS167* yield similar profiles of genetic "synthetic lethal" interactions when combined with mutations in genes encoding other cytoskeletal components. Mutations which specifically disrupt the SH3 domain-mediated interaction between Abp1p and Srv2p, however, show none of the shared phenotypes of *abp1* and *rvs167* mutations. We conclude that the Abp1p SH3 domain mediates the association of Srv2p with the cortical actin cytoskeleton, and that Abp1p performs a distinct function that is likely to involve binding by the Rvs167p SH3 domain. Overall, work presented here illustrates how SH3 domains can integrate the activities of multiple actin cytoskeleton proteins in response to varying environmental conditions.

INTRODUCTION

The dynamic regulation of the membrane actin cytoskeleton is of central importance in processes such as cell locomotion and migration, cell adhesion, endocytosis, and polarized secretion (Kubler and Riezman, 1993; Drubin and Nelson, 1996; Gumbiner, 1996; Lauffenburger and Horwitz, 1996; Mitchison and Cramer, 1996). Although scores of proteins which bind to actin directly or associate with actin indirectly have been identified (Stossel *et al.*, 1985; Pollard and Cooper, 1986; Sun *et al.*, 1995), understanding of the functions of these proteins and how they are coordinately regulated is far from complete. In view of the wide range of cellular processes in which actin has been implicated and of the number of signaling pathways that influence the actin cytoskeleton, it is not surprising that an increasingly complex picture of the physical and functional interactions among actin-associated proteins is emerging (Noegel and Luna, 1995; Sullivan and Therkauf, 1995; Ayscough and Drubin, 1996).

Study of the membrane actin cytoskeleton in *Saccharomyces cerevisiae* is facilitated by the apparent simplic-

* Corresponding author.

ity of the cytoskeleton and by the sophisticated genetic analysis possible in this organism. Yeast homologues of many actin-binding proteins found in other species, including cofilin, fimbrin, tropomyosin, profilin, and a heterodimeric actin filament capping complex (Cap1p/Cap2p), have been characterized (reviewed by Welch *et al.*, 1994; Ayscough and Drubin, 1996). Novel genetic screening procedures have also led to the discovery of other actin-associated proteins first or exclusively in *S. cerevisiae*. The likelihood that principles which emerge from the study of proteins in this second category will be relevant to organisms other than yeast is supported by the fact that yeast cytoskeletal proteins such as Sla2p, Abp1p, and Rvs167p show amino acid sequence similarity with proteins in *Caenorhabditis elegans* and vertebrates (see below and DISCUSSION).

Features common to some actin-associated proteins in a range of organisms from vertebrates to yeasts are the presence of SH3 domains and/or amino acid sequences similar to known SH3 domain-binding sites. SH3 domains are regions of about 50–60 amino acids which bind to short proline-rich regions of their ligands (see Mayer and Eck, 1995, and the references therein). Vertebrate actin-associated proteins containing SH3 domains include proteins with structural roles such as fodrin and nebulin (Merilainen *et al.*, 1993; Wang *et al.*, 1996), unconventional myosins (Bement *et al.*, 1994; Stoffler *et al.*, 1995; Goodson *et al.*, 1996), kinases and associated molecules (Flynn *et al.*, 1993; Turner and Miller, 1994; Hildebrand *et al.*, 1996), and other actin-binding proteins such as cortactin (Wu and Parsons, 1993). In *S. cerevisiae*, SH3-containing proteins include the actin-associated proteins Abp1p (Drubin *et al.*, 1990), Sla1p (Holtzman *et al.*, 1993), and Rvs167p (Bauer *et al.*, 1993), as well as Bem1p and the recently identified Boi1p and Boi2p, which have roles in the maintenance of normal cellular and cytoskeletal morphology (Chenevert *et al.*, 1992; Bender *et al.*, 1996; Matsui *et al.*, 1996). A number of yeast proteins implicated in cytoskeletal function, including Abp1p, Sla1p, Boi1p, Boi2p, and Srv2p (Field *et al.*, 1990), contain proline-rich regions which include amino acid sequences similar to known binding sites for SH3 domains. The presence of SH3 domains and potential SH3 domain-binding sites among proteins that are physically and/or functionally associated with actin suggests that SH3 domains may mediate the formation of specific protein complexes that underlie the complex architecture and regulation of the actin cytoskeleton.

Abp1p (actin-binding protein) was first identified by actin filament affinity chromatography and was subsequently shown to localize to the cortical actin cytoskeleton ("actin patches") in vivo (Drubin *et al.*, 1988). Null mutations in the *ABP1* gene do not cause obvious cellular growth or cytoskeletal defects, and the molecular functions of Abp1p are not yet fully understood. Abp1p shares regions of sequence similarity with *Dictyostelium* coactosin (de Hostos *et al.*, 1993) and the vertebrate actin-binding protein drebrin (see DISCUSSION), and the known properties and domain structure of Abp1p bear resemblance to vertebrate cortactin (Wu and Parsons, 1993). Abp1p and cortactin both contain a single C-terminal SH3 domain and an N-terminal actin-binding domain. The SH3 domain of Abp1p has recently been shown to bind specifically in vitro to a proline-rich segment of the Srv2 protein, and Srv2p, like Abp1p, localizes to the cortical actin patches (Freeman *et al.*, 1996).

Srv2p and its vertebrate homologues have been shown to bind monomeric actin (Gieselmann and Mann, 1992; Freeman *et al.*, 1995), and Srv2p in budding yeast has been implicated in the transmission of cyclic AMP- (cAMP) mediated signals via the *RAS*/adenylyl cyclase pathway (Fedor-Chaiken *et al.*, 1990; Gerst *et al.*, 1991; Wang *et al.*, 1993). The possible physical linkage of Abp1p to the *RAS*/adenylyl cyclase pathway via Srv2p suggests that Abp1p may function in the control of the actin cytoskeleton in response to varying nutritional conditions or environmental stresses. Several proteins in addition to Srv2p seem likely to have functions closely related to that of Abp1p. Like Abp1p and Srv2p, Sla1p (synthetic lethal-*ABP1*), Sla2p, and Sac6p (yeast fimbrin) coimmunolocalize in the cortical actin cytoskeleton (Drubin *et al.*, 1988; Adams *et al.*, 1989; Lila, Yang, and Drubin, unpublished observations) and were identified in a screen for strong genetic enhancers of an *ABP1* null mutation (synthetic lethals; Holtzman *et al.*, 1993). Rvs167p interacts with actin in the yeast two-hybrid system (Amberg *et al.*, 1995), and has functions important for sporulation and viability under adverse growth conditions (Bauer *et al.*, 1993). Rvs167p and Sla1p also contain one and three SH3 domains, respectively, suggesting that they too may interact physically with other cytoskeletally associated proteins.

Important tasks are to determine what physical interactions occur among actin-associated proteins in vivo and to determine the functions of these interactions by examining the phenotypic effects of mutations which disrupt them. Here, we report the results of genetic, phenotypic, and immunocytological analysis of the Abp1p/Srv2p SH3 domain-mediated interaction in vivo. We demonstrate that the SH3 domain of Abp1p mediates the cytoskeletal subcellular localization of Srv2p, but that this function of Abp1 is genetically distinct from another function(s) of the protein. A survey of other potential SH3 domain-mediated interactions among yeast actin-associated proteins shows that the Rvs167p SH3 domain binds to Abp1p. Other evidence presented indicates that this property of Abp1p provides a likely mechanistic basis for phenotypes and genetic interactions associated with *ABP1*

mutation. Abp1p, Srv2p, and Rvs167p are here or have previously all been shown to have functions important for cellular responses to poor or changing growth media. Overall, our results suggest that SH3 domain-mediated complexes are important for integrating the activities of actin-associated proteins to suit varying environmental conditions.

MATERIALS AND METHODS

Media and Yeast Strain Manipulations

Yeast strains used in these studies are listed in Table 1. Standard growth and sporulation media were used and are described by Rose *et al.* (1990). Medium used for *URA3* plasmid counterselection (Boeke *et al.*, 1987) contained 1 mg/ml 5-fluoroorotic acid (5-FOA, American Bioorganics, Niagara Falls, NY) and 5 mg/l uracil. Cell viability was determined by serial dilution of cultures in distilled water followed by mild sonication and plating on YPD-agar medium. Colonies were counted after 3 d of growth at 25°C. Sporulation efficiency was assessed by phase-contrast microscopic examination of sporulated cultures. Yeast transformations were performed using lithium acetate as described by Ito *et al.* (1983).

SRV2 *Gene Disruption*

Replacement of the *SRV2* gene nucleotides −3 to 797 relative to the translation start site codon with a 1.6-kb DNA fragment containing the *HIS3* gene was performed using a polymerase chain reaction-(PCR) based strategy (Baudin *et al.*, 1993). Forward primer 5′-ttt cgt aat tga gta ggc caa gtt gca acc gtg tga aat cga ttg tac tga gag tgc acc-3′ and reverse primer 5′-act gtg cgt cgt cct tga aat ctg tga cca tag aca cgg gag tgc ggt att tca cac cgc-3′ were used with plasmid pRS306 (Sikorski and Hieter, 1989) as a template to generate a 1.6-kb PCR product containing the *HIS3* gene and with 42 5′ nucleotides and 44 3′ nucleotides homologous to *SRV2*. This PCR product was used to transform a wild-type diploid strain and genomic DNA prepared from the resultant transformants. An *SRV2* disruptant was identified by the presence of a unique 700-bp PCR product from a reaction using 1 μl of this genomic DNA as a template and *HIS3* homologous forward primer 5′-agt gcg ttc aag gct ctt gcg-3′ and reverse primer 5′-cgc cga att ccc tac caa ttc ctt tct agg-3′, which is complementary to *SRV2* sequences. The *HIS3* sense strand is in the same orientation as that of *SRV2* in the *srv2Δ2* disruption.

DNA Manipulations and PCR

Plasmids used in these studies and the strategies used in their construction are described below. Standard techniques were used for plasmid isolation, analysis, and restriction fragment cloning (Sambrook *et al.*, 1989). PCR (Innis *et al.*, 1990) was performed in 100-μl reactions using Vent polymerase (New England Biolabs, Beverly, MA) under conditions recommended by the manufacturer and an M.J. Research PTC100 thermal cycler. Where two-step PCR is indicated in the construction of plasmid deletions and chimeric DNA molecules, desired DNA fragments 5′ and 3′ of the intended deletion or chimera junction were amplified in separate PCRs using primers that resulted in at least 20 nucleotides of homology between the two products spanning the junction. The two PCR products were then purified from agarose gels using the Geneclean kit (BIO 101, La Jolla, CA), and approximately 10^7 molecules of each purified product were combined to serve as the template DNA for the second step PCR reaction. DNA sequencing was accomplished by means of the dideoxy nucleotide chain termination method using Sequenase (U.S. Biochemical, Cleveland OH) DNA polymerase and conditions recommended by the manufacturer.

Plasmids

The following plasmids were used: pNF275: YCp50 vector (Rose *et al.*, 1987); a 10-kb genomic fragment carrying SRV2 cloned as an Sau3A partial digest fragment of *S. cerevisiae* strain SP1 genomic DNA in the *Bam*HI site of the vector (obtained from N. Freeman and J. Field, University of Pennsylvania, Philadelphia, PA).

pTL102: 1.3-kb SRV2-coding sequence *Pst*I/*Eco*RI fragment cloned in a KS+ Bluescript vector.

pSRV2–1: pRS315-based (Sikorski and Hieter, 1989) plasmid with 3.4-kb SRV2-containing *Hin*dIII fragment from pNF275 cloned into pRS315. Isolate "a" 5′ end is closest to the *Sac*I site of the vector, isolate "b" is in opposite orientation.

pDD210: pRS316 vector, otherwise identical to pSRV2–1b.

pSRV2–2: pSRV2–1 derivative with sequences encoding amino acids 354–358 deleted. Constructed by M13 oligonucleotide-directed mutagenesis (Sambrook *et al.*, 1989) using pSRV2–1a-derived single-stranded DNA template and primer SRV8 (5′-gta aat ccg gta aaa agc cat caa cat tga aa-3′).

pSRV2–3: pSRV2–1 derivative in which sequences encoding the Abp1p SH3 domain-binding site (Srv2p amino acids 352–360, ... SGPPPRPKK...) have been altered to encode an amino acid sequence which matches a consensus chicken cSrc SH3 domain-binding site (RGLPPLPRF). Two-step PCR construction strategy: 5′ PCR product-pSRV2–1b template using forward primer BS1 (5′-cga gga atg ttg cgt cag gag cac-3′) and reverse primer SRV4 (5′-tgg caa tgg tgg tag acc cct ttt act tcc tgt -3′). 3′ PCR product- pSRV2–1a template using forward primer SRV3 (5′-ggt cta cca cca ttg cca aga ttt cca tca aca ttg-3′) and reverse primer BS1. Products were mixed and a 3.5-kb product amplified using primer BS1. Product was cloned as *Hin*dIII fragment into pRS315.

pSRV2–4: pSRV2–1 derivative, sequences encoding amino acids 267–285 deleted. Two-step PCR construction strategy: 5′ PCR product-pTL102 template, forward primer BS1, reverse primer SRV9 (5′-gac gga agc aga tga agt agc acc tgt att-3′), 3′ PCR product-pSRV2–1b template, forward primer SRV10 (5′-gct act tca tct gct tcc gtc ttt gaa atc tc-3′), reverse primer SRV2 (5′-cgc cga att ccc tac caa ttc ctt tct agg-3′). Products were mixed, and a 1080-bp fragment was amplified with primers BS1 and SRV2. Product was cloned as a *Nsi*I/*Stu*I fragment into gel-purified vector fragment of *Nsi*I/*Stu*I-digested pSRV2–1b.

pSRV2–5: pSRV2–1 derivative, sequences encoding amino acids 267–285 and 354–358 deleted. Two-step PCR construction strategy: 5′ PCR product- pTL102 template, forward primer BS1, reverse primer SRV9. 3′ PCR product-pSRV2–3 template, forward primer SRV10, reverse primer SRV2. Products were mixed, and a 1080-bp fragment was amplified with primers BS1 and SRV2. Product was cloned as a *Nsi*I/*Stu*I fragment into gel-purified vector fragment of *Nsi*I/*Stu*I-digested pSRV2–1b.

pSRV2–6: pSRV2–1 derivative with sequences encoding amino acids 169–368 deleted. Constructed by recircularization of pSRV2–1b digested with *Eco*47III and *Stu*I.

pSRV2–7: pSRV2–1 derivative with sequences encoding amino acids 169–262 deleted. PCR product from reaction with pSRV2–1b template and forward primer SRV11 (5′-act tca tct cct tcg cca gc-3′), reverse primer SRV2, was gel purified, 5′ phosphorylated with T4 polynucleotide kinase (United States Biochemical, Cleveland, OH), digested with *Stu*I, and cloned into a gel-purified vector fragment of *Eco*47III/*Stu*I-digested pSRV2–1b.

pGABP1–1: pGEX3X (Pharmacia, Piscataway, NJ) derivative. Directs expression of Abp1p amino acids 535–592 (SH3 domain) as glutathione *S*-transferase (GST) fusion in *Escherichia coli*. PCR product from reaction using forward primer ABP5 (5′-gcc aaa ggg gat ccc ttg ggc cac agc-3′); reverse primer ABP6 (5′-gac gct gac ggg atc ctc tag ttg ccc-3′) was cloned as *Bam*HI fragment into pGEX3X.

pGSLA1–1: pGEX3X (Pharmacia) derivative. Directs expression of Sla1p amino acids 8–64 (SH3 domain 1) as GST fusion in *E. coli*. PCR product from reaction using forward primer SLA5 (5′-cgc ggg atc cca tgg tat agg gcc gtc tat gcc-3′); reverse primer SLA6 (5′-cgc cga

Table 1. Yeast strains

Designation	Genotype	Source
DDY321	MATa *ura3-52 his3Δ200 leu2-3,112 Δabp1::LEU2*	Drubin laboratory
DDY898	MATa *ura3-52 his3Δ200*	Drubin laboratory
DDY991	MATa/α *ura3-52/ura3-52 leu2-3,112/leu2-3,112 his3Δ200/+lys2-801am/+trp1-1/trp1-1 abp1::LEU2/+rvs167::TRP1/+*	This study
DDY992	MATa/α *ura3-52/ura3-52 leu2-3,112/leu2-3,112 his3Δ200/+lys2-801am/+ trp1-1/trp1-1 sla1::URA3/+ rvs167::TRP1/+*	This study
DDY993	MATa/α *ura3-52/ura3-52 leu2-3,112/leu2-3,112 his3Δ200/his3Δ200 lys2-801am/+ trp1-1/ trp1-1 sac6::URA3/+ rvs167::TRP1/+*	This study
DDY994	MATa/α *ura3-52/ura3-52 leu2-3,112/leu2-3,112 his3Δ200/his3Δ200 lys2-801am/+ trp1-1/ trp1-1 sla2::URA3/+ rvs167::TRP1/+*	This study
DDY995	MATα *ura3-52 his3Δ200 leu2-3,112 lys2-801am sla1-7 abp1::LEU2* (pRS316/SLA1$^+$)	This study
DDY996	MATa *ura3-52 his3Δ200 leu2-3,112 ade2-1 sla2-5 abp1::LEU2* (pDD13 URA3$^+$ ABP1$^+$)	This study
DDY997	MATa *ura3-52 his3Δ200 leu2-3,112 ade2-1 sac6-102 abp1::LEU2* (pDD13 URA3$^+$ ABP1$^+$)	This study
DDY998	MATa *ura3-52 his3Δ200 leu2-3,112 lys2-801am ABP1$^+$:HIS3*	This study
DDY999	MATa *ura3-52 his3Δ200 leu2-3,112 lys2-801am abp1^{Src}:HIS3*	This study
DDY1000	MATa *ura3-52 his3Δ200 leu2-3,112 lys2-801am abp1::LEU2*	This study
DDY1003	MATα *ura3-52 his3Δ200 leu2-3,112 lys2-801am* (pRS315)	This study
DDY1004	MATα *ura3-52 his3Δ200 leu2-3,112 lys2-801am srv2Δ2::HIS3* (pRS315)	This study
DDY1005	MATα *ura3-52 his3Δ200 leu2-3,112 lys2-801am srv2Δ2::HIS3* (pSRV2-1)	This study
DDY1006	MATα *ura3-52 his3Δ200 leu2-3,112 lys2-801am srv2Δ2::HIS3* (pSRV2-3)	This study
DDY1007	MATa/α *ura3-52/ura3-52 leu2-3,112/leu2-3,112 his4-619/+ his3Δ200/+ abp1::LEU2/abp1:: LEU2*	This study
DDY1008	MATa/α *his4-619/+ his3Δ200/+*	This study
DDY1009	MATa/α *his3Δ200/his3Δ200 leu2-3,112/+ ura3-52/+ lys2-801am/+ srv2Δ2::HIS3/+*	This study
DDY1010	MATa/α *ura3-52/ura3-52 leu2-3,112/leu2-3,112 his3Δ200/his3Δ200 srv2Δ2::HIS3/+ abp1:: LEU2/+*	This study
DDY1011	MATa/α *ura3-52/ura3-52 leu2-3,112/leu2-3,112 his3Δ200/his3Δ200 lys2-801am/+ trp1-1/+ srv2Δ2::HIS3/+ sac6::URA3/+*	This study
DDY1012	MATa/α *ura3-52/ura3-52 leu2-3,112/leu2-3,112 his3Δ200/his3Δ200 lys2-801am/+ lys9/+ srv2Δ2::HIS3/+ sla1::URA3/+*	This study
DDY1013	MATa/α *ura3-52/ura3-52 leu2-3,112/leu2-3,112 his3Δ200/his3Δ200 lys2-801am/+ srv2Δ2:: HIS3/+ sla2Δ1::URA3/+*	This study
DDY1014	MATa/α *ura3-52/ura3-52 leu2-3,112/leu2-3,112 his3Δ200/his3Δ200 trp1-1/trp1-1 rvs167:: TRP1/+ srv2Δ2::HIS3/+*	This study
DDY1015	MATα *ura3-52 leu2-3,112 his3Δ200 trp1-1 lys2-801am rvs167::TRP1*	This study
DDY1016	MATα *ura3-52 leu2-3,112 trp1-1 abp1::LEU2*	This study
DDY1018	MATa *ura3-52 leu2-3,112 trp1-1 his3Δ200 lys2-801am*	This study
DDY1019	MATα *ura3-52 leu2-3,112 his3Δ200 lys2-801am ade2-1 sla2-5 srv2Δ2::HIS3* (pRS316/SRV2$^+$)	This study
DDY1020	MATα *ura3-52 leu2-3,112 his3Δ200 ade2-1 sac6-102 srv2Δ2::HIS3* (pRS316/*SRV2*$^+$)	This study
DDY1021	MATa *ura3-52 leu2-3,112 his3Δ200 trp1-1 srv2Δ2::HIS3 rvs167::TRP1* (pRS316/*SRV2*$^+$)	This study
DDY1022	MATa/α *ura3-52/ura3-52 leu2-3,112/leu2-3,112 his3Δ200/his3Δ200 lys2-801am/+ srv2Δ2:: HIS3/srv2Δ2::HIS3*	This study
DDY1103	MATa *ura3-52 leu2-3,112 his3Δ200 lys2-801am abp1^{S7A14S}:HIS3*	This study
DDY1091	MATa/α *ura3-52/ura3-52 leu2-3,112/leu2-3,112* his4-619/+ *his3Δ200/+ Δabp1::LEU2/Δabp1::LEU2* (pRS316)	This study
DDY1092	MATa/α *ura3-52/ura3-52 leu2-3,112/leu2-3,112* his4-619/+ *his3Δ200/+ Δabp1::LEU2/Δabp1::LEU2* (pRS316/*ABP1*)	This study
DDY1094	MATa/α *ura3-52/ura3-52 leu2-3,112/leu2-3,112 his3Δ200/his3Δ200 lys2-801am/+ srv2Δ2:: HIS3/srv2Δ2::HIS3* (pRS315)	This study
DDY1095	MATa/α *ura3-52/ura3-52 leu2-3,112/leu2-3,112 his3Δ200/his3Δ200 lys2-801am/+ srv2Δ2:: HIS3/srv2Δ2::HIS3* (pSRV2-1)	This study
DDY1096	MATa/α *ura3-52/ura3-52 leu2-3,112/leu2-3,112 his3Δ200/his3Δ200 lys2-801am/+ srv2Δ2:: HIS3/srv2Δ2::HIS3* (pSRV2-2)	This study
LG430	MATa *trp1-1 rvs167::TRP1* Parent strain for *RVS167* disruptions used in these studies	M. Aigle

att cgc atg cta gta agt gga ggg cac tag acc-3′) was cloned as *Bam*HI/*Eco*RI fragment into pGEX3X.

pGSLA1–2: pGEX3X (Pharmacia) derivative. Directs expression of Sla1p amino acids 74–131 (SH3 domain 2) as GST fusion in *E. coli*. PCR product from reaction using forward primer SLA7 (5′-gcg gga tcc cat ggg taa gag cca ttt atg-3′); reverse primer SLA8 (5′-cgc cgg atc cgc atg cta att ctc tgg ttc gac gta-3′) was cloned as *Bam*HI/*Eco*RI fragment into pGEX3X.

pGSLA1–3: pGEX3X (Pharmacia) derivative. Directs expression of Sla1p amino acids 358–414 (SH3 domain 3) as GST fusion in *E. coli*. PCR product from reaction using forward primer SLA9 (5′-cgc gga tcc cat ggg gta ttg ttc aat atg ac-3′); reverse primer SLA10 (5′-cgc

cga att cgc atg cta acg aac agg ctc aat aaa c-3′) was cloned as *Bam*HI/*Eco*RI fragment into pGEX3X.

pGSRC-1: pGEX3X (Pharmacia) derivative. Directs expression of chicken cSRC amino acids 86–141 (SH3 domain) as GST fusion in *E. coli*. PCR product from reaction using chicken cSrc plasmid DNA template, forward primer DH7 (5′-gca cca tgg ttc gtg gct ctc tac gac-3′); reverse primer SRC1 (5′-ctg cgg ccg cat gct agt ctg agg gcg cga cat ag-3′) was cloned as *Nco*I/*Sph*I fragment into a gel-purified vector fragment of *Nco*I/*Sph*I-digested pGSLA1–2.

pGS7A14S: pGEX3X (Pharmacia) derivative. Directs expression of chimeric SH3 domain. A 160-bp *Nco*I/*Sph*I fragment from pS7A14S (see below) was cloned into a gel-purified vector fragment of *Nco*I/*Sph*I-digested pGSLA1–2.

pGRVS-1: pGEX3X (Pharmacia) derivative. Directs expression of Rvs167p amino acids 426–482 as GST fusion in *E. coli*. PCR product from reaction using pUKC200–9 (Bauer *et al.*, 1993) template, forward primer RVS1 (5′-cgc ggg atc ccc gaa act gtt acc gca ttg tat-3′); reverse primer RVS2 (5′-ggg cga att cta gtt ctt gtt gag ttg cac-3′) was cloned as *Bam*HI/*Eco*RI fragment into *Bam*HI/*Eco*RI-digested pGEX3X.

pGABP1–2: pGEX3X (Pharmacia) derivative. Directs expression of Abp1p proline-rich region, amino acids 444–537, as GST fusion in *E. coli*. PCR product from reaction using forward primer ABP7 (5′-ggg gga tcc atg aag acg agg ctg ctc aac c-3′); reverse primer ABP8 (5′-gcg gat ccc tga att cca agg att ttc ctt tgg c-3′) was cloned as *Bam*HI/*Eco*RI fragment into pGEX3X.

pGSRV2–1: pGEX3X (Pharmacia) derivative. Directs expression of Srv2p amino acids 337–368 as a GST fusion protein in *E. coli*. PCR product from reaction using pSRV2–1 template, forward primer SRV1 (5′- gtc gcg gat ccc tga att acg tca atc c-3′); reverse primer SRV2 was cloned as *Bam*HI/*Eco*RI fragment into pGEX3X.

pGSRV2–2 (pDD205): As above, but deleted for sequences encoding Srv2p amino acids 354–358. Constructed as above, except that the pSRV2–2 template was used for PCR.

pGSRV2–3 (pDD206): Similar to pGSRV2–1, except that the Abp1p SH3-binding site mutated to match cSrc consensus. Constructed as above, except that the pSRV2–3 template was used for PCR.

pDD215: pGEX1 (Pharmacia) derivative containing genomic *Eco*RI fragment from *SLA1*. Directs expression of Sla1p amino acids 117–511 as GST fusion protein in *E. coli*.

pABP1$^+$: A 3.5-kb genomic *Eco*RI fragment carrying *ABP1*$^+$ in pRS315 vector, and with *HIS3* gene inserted into *Sna*BI site in *ABP1* 3′ noncoding region; 1.6-kb *Bam*HI fragment from pJJ215 filled in with Klenow polymerase (Boeringer Mannheim, Indianapolis, IN) and blunt end ligated into *Sna*BI site. *HIS3* and *ABP1* are transcribed in same direction, 5′ end of sense strand is closest to *Sac*I site of vector.

pDD3: A 3.5-kb *Eco*RI fragment carrying *ABP1* cloned in YEp420 vector.

pABP1-Δ1: pABP1$^+$-based plasmid, encodes truncated Abp1p missing amino acids 536–592. PCR product 1 from reaction using pABP1–1 template, forward primer ABP1 (5′-cga gga agt ttg cgt cag gag cac-3′); reverse primer ABP2 (5′-gct gca tgc taa gga ttt tcc ttt ggc-3′) was digested with *Xba*I + *Sph*I. PCR product 2 from reaction using pABP1–1 template, forward primer ABP3 (5′-gtg cat gcg ggc aac tag aat cac acg-3′); reverse primer BS1 was digested with *Apa*I + *Sph*I. Restricted PCR products were combined with a gel-purified pABP1$^+$ vector fragment from *Apa*I/*Xba*I partial digest and ligated.

pTL5: pABP1+ derivative, contains engineered unique *Nco*I and *Sph*I restriction sites in place of SH3 domain-coding sequences to allow for heterologous SH3 domain substitution. PCR product from reaction using pABP1–1 template, forward primer ABP1; reverse primer ABP9 (5′-gga tca tag cat gct gtg gcc cat gga ttt tcc-3′) was digested with *Xba*I and *Sph*I and cloned into *Xba*I/*Sph*I sites of a gel-purified vector fragment from pABP1–2 partial digest.

pABP1-Src: pTL5 derivative, contains chicken cSrc SH3 domain amino acid 86–141 coding sequences. PCR product from reaction using cloned chicken cSrc plasmid DNA template, forward primer DH7 (5′-gca cca tgg ttc gtg gct ctc tac gac-3′); reverse primer SRC1 (5′-ctg cgg ccg cat gct agt ctg agg gcg cga cat ag-3′) was cloned as *Nco*I/*Sph*I fragment into a gel-purified vector fragment of *Nco*I/*Sph*I-digested pTL5.

pA14S: pTL5 derivative, contains chimeric SH3 domain sequences from Abp1p and cSrc domains. Two-step PCR construction strategy: 5′ PCR product- pABP1$^+$ template, forward primer ABP1, reverse primer A14S-R (5′-cgt tct cct ttc ttg aag gac agt tcg tta tct tct gc-3′). 3′ PCR product- chicken cSrc plasmid template, forward primer A14S-F (5′-tgt cct tca aga aag gag aac g-3′), reverse primer SRC1(5′-ctg cgg ccg cat gct agt ctg agg gcg cga cat ag-3′). Products were mixed, and a 340-bp product was amplified with forward primer ABP1, reverse primer SRC1. Product digested with *Nco*I + *Sph*I and cloned into pTL5.

pS7A14S: pA14S derivative. PCR product from reaction with pA14S template, forward primer S7A-F (5′-cct ttt agg tac caa gca ccg tga tat act aat gct gcg ac-3′); reverse primer SRC1 was digested with *Nco*I + *Sph*I and cloned into pTL5.

Immunofluorescence Microscopy

Yeast cultures were grown in SD medium to OD_{600} of 0.1–0.2 and processed for immunofluorescence as described (Pringle *et al.*, 1989, 1991). Srv2p localization was achieved using affinity-purified rabbit polyclonal antiserum JF155 raised against full-length Srv2p (gift from Dr. J. Field, University of Pennsylvania). Rabbit polyclonal anti-Abp1p antibodies were affinity purified as described (Harlow and Lane, 1988a) using an affinity matrix of 1 ml of swollen cyanogen bromide-Sepharose beads (Pharmacia), to which 2 mg of a GST protein fusion to Abp1p amino acids 12–592 had been coupled. Antibodies were eluted from the matrix with 4.5 M MgCl, dialyzed into phosphate-buffered saline plus 30% glycerol, and stored at −20°C. For actin double-labeling experiments, affinity-purified anti-Abp1p or Srv2p sera at a 1:50 dilution and a guinea pig anti-yeast actin serum (gift from D. Botstein) at a 1:1000 dilution were used. Secondary antibodies were used at a 1:1000 dilution and were rhodamine-conjugated goat anti-rabbit IgG and fluorescein-conjugated goat anti-guinea pig IgG for double-label experiments, and fluorescein-conjugated goat anti-rabbit IgG for single label experiments (Cappel/Organon Teknika, Malvern PA). Slides were viewed and photographed using a Zeiss Axiophot microscope.

E. coli *Whole-Cell Extract Production*

Recombinant protein expression plasmids were propogated in *E. coli* strain HB101. Cells were grown in LB medium with 75 μg/ml ampicillin at 37°C to OD_{600} of 0.2. Recombinant protein expression was induced by addition of isopropyl-thio-β-D-galactopyranoside (Sigma, St. Louis MO) to 0.1 mM and further incubation for 4 h. Cells (1 ml) were then centrifuged and resuspended in 150 μl of 50 mM sodium phosphate (pH 7.5)/150 mM NaCl. Twice concentrated SDS-polyacrylamide gel sample buffer (150 μl) was added, and the samples were heated for 5 min in boiling water. Samples of 5 μl were run per lane on SDS-7% polyacrylamide gels. Proteins were transferred to nitrocellulose membranes as described (Harlow and Lane, 1988b).

SH3 Domain Probes

SH3 domain fusions to GST were purified by glutathione agarose (Sigma) affinity as described (Ausubel, 1990). Purified protein was exchanged into 0.1 M sodium borate (pH 8.8) by gel filtration and biotinylated by adding 60 μg of biotinamidocaproate succinimide ester (Sigma) per mg of protein and incubating for 4 h at room temperature. NH_4Cl (100 μl, 1 M) was added per mg of protein, and the labeled probe exchanged into phosphate-buffered saline (pH 7.5) plus 10% glycerol. Aliquots were frozen in liquid nitrogen and stored at −20°. Probing of blots of candidate ligands was performed as described (Cicchetti *et al.*, 1992). Probes were allowed to bind for

4 h at 4 °C and used at a concentration of 1 μg/ml. Detection was accomplished by a 1-h incubation at 4°C with a 1:5000 dilution of alkaline phosphatase-conjugated streptavidin (Boeringer Mannheim), followed by washing and addition of 5-bromo-4-chloro-3-indolyl-phosphate and nitroblue tetrazolium as recommended by the supplier (Promega, Madison WI).

Amino Acid Similarity Comparisons

Amino acid sequence similarities between Abp1p and drebrins were identified using the BLAST algorithim (Altschul *et al.*, 1990) made available by the National Center for Biotechnology BLAST server (http://www.ncbi.nlm.nih.gov/BLAST/). An amino acid query missing the SH3 domain was submitted against the GenBank non-redundant protein sequence database using the PAM250 amino acid substitution matrix. Optimal alignment of the Abp1p and rat drebrin A (National Center for Biotechnology identifier gi/297821) sequences was performed using the FASTA-based (Pearson and Lipman, 1988) ALIGN tool available at EERIE, France (http://genome.eerie.fr/fasta/align-query.html). Proteins containing regions similar to the Srv2p SH3 domain-binding site were identified by a FASTA search of the *S. cerevisiae* non-redundant protein database at Stanford University (http://genome-www.stanford.edu/*Saccharomyces*/).

RESULTS

SH3 Domain-mediated Interactions among Actin-associated Proteins

The presence of both SH3 domains and proline-rich potential SH3 domain-binding sites in a number of *S. cerevisiae* actin-associated proteins led us to conduct a survey of potential binding interactions among selected proteins implicated in cytoskeletal function. Protein probes corresponding to the SH3 domains of Abp1p, Rvs167p, and each of the three Sla1p SH3 domains were assayed for binding to a panel of bacterially produced proteins or protein fragments which included proline-rich regions of Abp1p, Sla1p, Srv2p, Boi1p, Boi2p, and the mammalian cAbl SH3 ligand 3BP1 (Cicchetti *et al.*, 1992). Figure 1 shows that the Abp1p SH3 domain binds to Srv2p as reported previously, and does not obviously associate with any of the other proline-rich candidate ligands. The Rvs167p SH3 probe binds to a region of Abp1p spanning amino acids 444–573, and a clear difference in the specificity of this probe as compared with the Abp1p SH3 probe is evident. No specific binding to any of the candidate ligands was detected for any of the Sla1p SH3 probes.

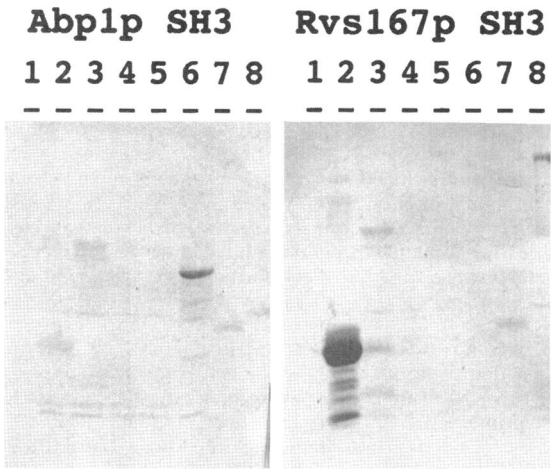

Figure 1. Binding of biotinylated GST-SH3 domain fusion protein probes to candidate ligands subjected to SDS-PAGE and transferred to nitrocellulose membranes. Duplicate blots of candidate ligands probed (see MATERIALS AND METHODS) with GST-Abp1p SH3 probe (left, pGABP1–1), or GST-Rvs167p SH3 probe (right, pGRVS-1). Bacterial lysates containing: lane 1, GST (pGEX3X); lane 2, GST-Abp1p amino acids 444–537 (pGABP1–2); lane 3, GST-Sla1p amino acids 118–511 (pDD215); lane 4, GST-Boi1p (pPB750; Bender *et al.*, 1996); lane 5, GST-Boi2p (pPB898; Bender *et al.*, 1996); lane 6, full-length Srv2p (pT7.CAP; Field *et al.*); lane 7, purified yeast actin; and lane 8, β-galactosidase-3BP1 (bacteriophage λgt11 3BP1 lysogen; Cicchetti *et al.*, 1992). Plasmids/phage used to direct expression of candidate ligands in *E. coli* appear in parentheses.

Abp1p SH3 Domain Mediates the Association of Srv2p with the Cortical Actin Cytoskeleton

We focus first on the interaction of Abp1p and Srv2p. Because Abp1p and Srv2p interact in vitro and colocalize in cortical actin patches, we determined whether Abp1p is required for the association of Srv2p with actin patches. Immunolocalization of Srv2p was performed in parallel in wild-type and *ABP1* deletion strains. No difference in the expression levels of Srv2p in whole-cell extracts prepared from growing cultures of the two strains could be detected by immunoblot analysis. Although the actin cytoskeleton is not noticeably perturbed by *ABP1* gene deletion (Drubin *et al.*, 1988), a difference in Srv2p fluorescence staining is apparent in *abp1* deletion strains as compared with wild type (Figure 2). The apparent loss of cortical actin patch association of Srv2p in *abp1* mutants is a reproducible effect in several different strain backgrounds. Several experiments demonstrated that loss of Srv2p localization is a specific consequence of disruption of the *ABP1* gene. First, the subcellular localizations of other cortical patch-associated proteins including actin, cofilin, and Sla1p are not noticeably affected by the *abp1* null mutation. Second, disruption of the *RVS167* (Figure 2), *SLA1*, *SLA2*, or *SAC6* genes does not result in loss of Srv2p cortical association. Abp1p was also found to localize to cortical actin patches in an apparently normal manner in *SAC6*, *SLA1*, *SLA2*, *SRV2*, and *RVS167* deleted strains. We conclude that the normal localization and/or stable association of Srv2p with cortical actin patch structures requires Abp1p.

If the association of Srv2p with the actin patches is dependent on direct interaction with the Abp1p SH3 domain, then mutant versions of Srv2p which lack the binding site for the Abp1p SH3 domain would also be expected to be deficient in cortical patch association. The binding of the Abp1p SH3 domain to Srv2p was previously shown to map to a 40-amino acid region

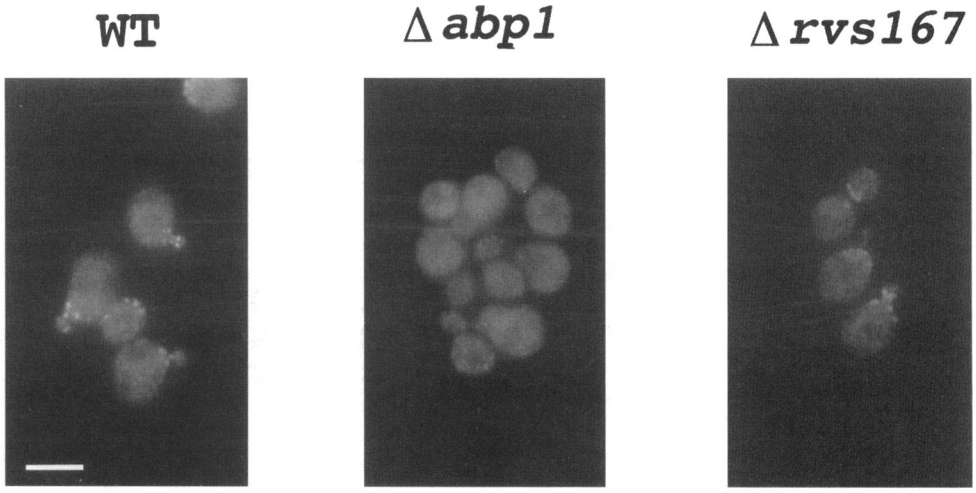

Figure 2. Immunofluorescence localization of Srv2p in strains bearing chromosomal disruptions in the indicated genes. Rabbit polyclonal antiserum JF155 (Freeman *et al.*, 1996) was used as described in MATERIALS AND METHODS. Strains are DDY1018 (left), DDY1016 (middle), and DDY1015 (right). Bar, 5 μm.

(residues 337–376) which contains one amino acid motif (KSGPPPRPKK) that is similar to known SH3 domain-binding peptides (Freeman *et al.*, 1996). Mutant versions of Srv2p containing deletions of large regions of the protein encompassing the above site had been shown to be deficient in actin patch association. These mutant proteins, however, fail to fully complement the morphological and cytoskeletal defects associated with *srv2* null mutations (Freeman *et al.*, 1996), limiting the interpretation of the subcellular localization experiments. We therefore sought to engineer mutations in *SRV2* that specifically abolish Abp1p SH3 domain binding and to examine the consequences of these mutations on Srv2p subcellular localization and on Srv2p function (see below).

To examine mutant Srv2 proteins without interference from the wild-type protein, it was first necessary to disrupt the *SRV2* gene in a strain of the S288C background used in our laboratory. The disruption inserts the *HIS3* auxotrophic marker gene in the place of nucleotides −3 to 797 relative to the first base of the start codon for *SRV2*. This gene disruption (referred to here as *srv2*Δ2) differs slightly from those generated previously which leave coding sequences for the first 76 amino acids intact. Results of tetrad analysis of a diploid strain heterozygous for the disruption are shown in Figure 3A. Previous phenotypic characterizations of *srv2* disruption phenotypes have included failure to grow on rich media (Fedor-Chaiken *et al.*, 1990; Field *et al.*, 1990). We do not observe this phenotype for the *srv2*Δ2 disruption (Figure 3A; see DISCUSSION). *HIS3*$^+$ segregants do show other phenotypes similar to those described for previous *srv2* gene disruptions such as a swollen, rounded cell morphology and poor growth at 37°C, and often yield slightly smaller colonies than their *his3* counterparts. No Srv2p could be detected in *srv2*Δ2 cell extracts by immunoblot analysis.

Mutations affecting the Srv2p SH3 domain-binding site were introduced into a plasmid bearing a genomic DNA fragment containing the *SRV2* gene (pSRV2–1). One mutation (in pSRV2–2) is expected to eliminate SH3 domain binding as it deletes Srv2p amino acids 354–358, which include the proline residues thought to be essential features of all SH3 domain-binding sites (Mayer and Eck 1995). A second mutation (in pSRV2–3) changes the binding site such that the predicted amino acid sequence matches a consensus sequence for peptides which bind to the cSrc SH3 domain (Yu *et al.*, 1994). Here, the Srv2p sequence has been changed from ... KSGPPPRPKK... to ... KRGLPPLPRF..., to match the peptide consensus of RXLPPLPRØ (Ø, any hydrophobic amino acid).

To verify that the *srv2* mutations have the intended effect on SH3 domain binding in vitro, bacterial GST fusion proteins to the 40-amino acid region of Srv2p containing the wild-type or mutant SH3 domain-binding sites were produced. Binding of bacterially produced GST fusions to the Abp1p and cSrc SH3 domains was assayed in a blot overlay assay. The results of these studies are shown in Figure 3B. The wild-type Srv2p SH3 domain-binding site is bound specifically by the Abp1p, but not the cSrc SH3 probe. As expected, deletion of critical prolines in the binding site results in no detectable binding above background by either SH3 probe, whereas mutating the binding site to match the cSrc-binding consensus results in preferential binding by the cSrc SH3 probe.

The effect of the SH3 domain-binding site mutations on cortical localization of the mutant Srv2 proteins is shown in Figure 3C. As expected, plasmid pSRV2–1, encoding wild-type Srv2p, produces a product which localizes to polarized cortical patches. However, the mutant protein containing the c-Src SH3-binding site consensus sequence (pSRV2–3) is not seen in association with cortical patches. Srv2p in which the critical

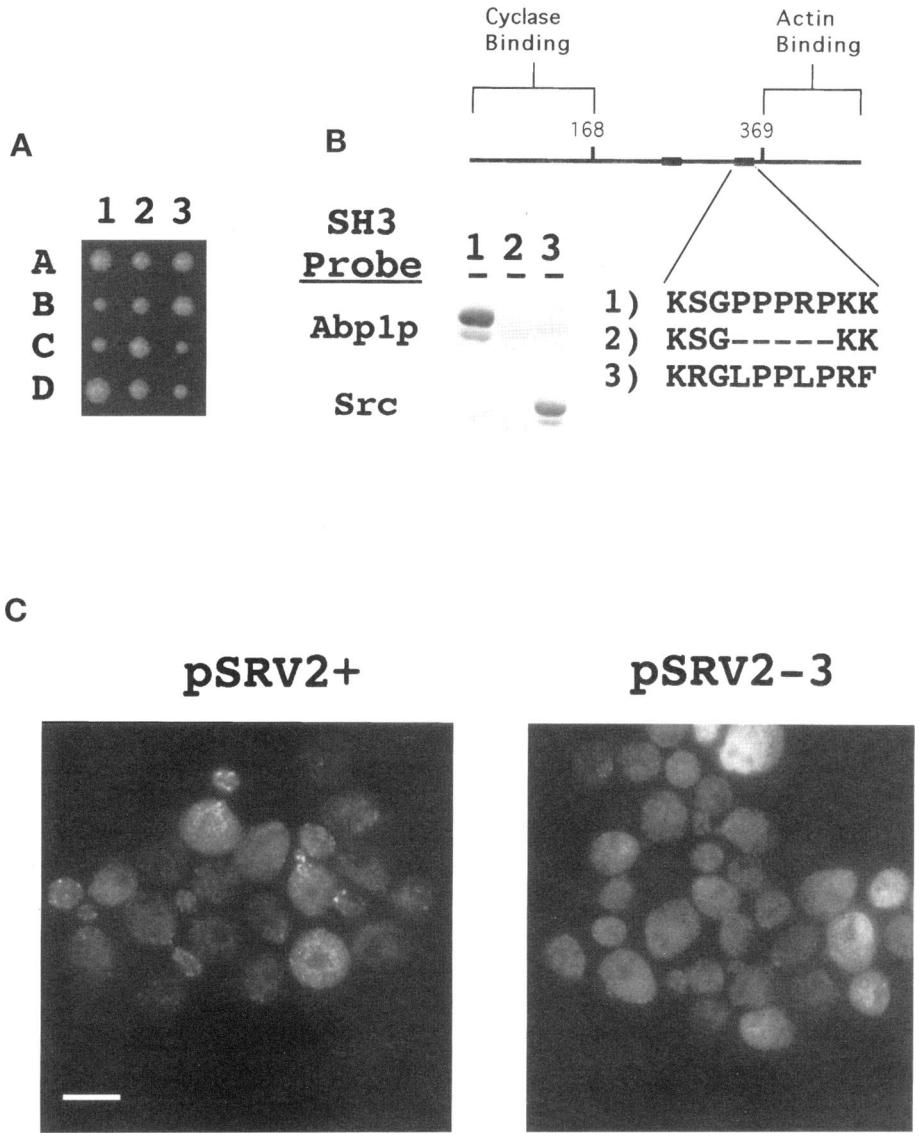

Figure 3. Effects of *SRV2* mutations on growth, SH3 domain binding, and Srv2p subcellular localization. (A) Growth of meiotic segregants from heterozygous *srv2*Δ*2* (see MATERIALS AND METHODS) strain DDY1009 after 4 d at 30°C on YPD medium. Segregants 1C, 1D, 2A, 2C, 3A, and 3D are *HIS3*$^+$ (*srv2*Δ *2*). (B) Protein fusions of Abp1p SH3 domain (top, pGABP1–1) or cSrc SH3 domain (bottom, pGSRC-1) were used to probe purified GST fusions to: lane 1, Srv2p amino acids 337–376 (pGSRV2–1); lane 2, Srv2p amino acids 337–376 with amino acids 354–358 deleted (pGSRV2–2); and lane 3, Srv2p amino acids 337–376 with the SH3 domain-binding site residues at positions 352–360 altered to conform with the consensus for peptides which bind to the cSrc SH3 domain (pGSRV2–3; see text for details). Plasmids used to direct expression of fusion proteins in *E. coli* appear in parentheses. (C) Immunofluorescence labeling of Srv2p in strains bearing a chromosomal disruption of the *SRV2* gene and carrying plasmids encoding wild-type Srv2p (pSRV2–1, strain DDY1005, left) and mutant Srv2p (pSRV2–3, strain DDY1006, right) in which the binding site for the Abp1p SH3 domain has been altered to match the consensus for peptides which bind to the cSrc SH3 domain (see text for details). Bar, 5 μm.

prolines of the SH3 domain-binding site are deleted (pSRV2–2) also fails to localize to cortical patches. This effect is obvious either in the haploid strains shown or in diploids, and is unlikely to be due to minor perturbations in Srv2p expression levels for several reasons. First, no difference in the amount of Srv2p produced by the three plasmids can be detected by immunoblot analysis. Second, Srv2p cortical localization is readily apparent either in diploid strains carrying only one copy of *SRV2*$^+$ or in strains which significantly overproduce Srv2p from a strong heterologous promoter (pADH-CAP$^+$; Gerst *et al.*, 1991).

To judge whether the effects of the Srv2p mutations described above are restricted to defects in SH3 domain binding (as opposed to the mutations having more global effects on Srv2p), we determined the ability of the mutant proteins to complement growth and morphological defects associated with *SRV2* gene disruption. Strain DDY1004, bearing the *srv2*Δ*2* chromosomal disruption and a control vector plasmid grows with a doubling time of approximately 4 h at 30°C in media selective for the plasmid auxotrophic marker, whereas an isogenic wild-type strain with the same vector plasmid (DDY1003) grows with a doubling time of 2.7 h. Plasmid pSRV2–1, containing the wild-type *SRV2* gene, and plasmid pSRV2–2, containing the SH3 domain-binding site deletion, were introduced into a strain bearing the *srv2*Δ*2* disruption. These strains (DDY1005 and DDY1006) were found to grow with doubling times of 2.5 and 2.6 h, respectively. Plasmids pSRV2–2 and pSRV2–3 (containing the c-Src SH3-binding consensus region in place of the Abp1

SH3 binding region) also behave indistinguishably from the wild-type control plasmid (pSRV2–1) in correcting other defects associated with the *srv2*Δ2 disruption examined, including the temperature-sensitive growth phenotype, cell morphology defects, and defects in organization of actin-containing structures as assessed by immunofluorescence microscopy. Thus, the Srv2p mutants defective in the SH3-binding site complement fully a variety of defects associated with the *srv2* null mutation. The above results demonstrate the specific requirement for Abp1p and for the Abp1p SH3 domain-binding site in Srv2p in the localization of Srv2p to the cortical actin patches. Taken together, these findings provide strong evidence that an in vivo function of Abp1p is to facilitate stable association of Srv2p with the cortical actin cytoskeleton.

Functional Analysis of the Abp1p/Srv2p Protein Complex Reveals That Abp1p Performs at Least Two Independent Functions

Srv2p is known have two functional domains (an actin-binding and an adenylyl cyclase-binding domain) in addition to the Abp1p SH3 domain-binding site (Gerst *et al.*, 1991; Mintzer and Field, 1994; Freeman *et al.*, 1995). Null mutations in *SRV2* cause phenotypic effects not seen in *abp1* null mutants; therefore, Srv2p must have functions that are independent of Abp1p. Nonetheless, the physical association of Abp1p and Srv2p suggests that the two proteins participate in at least one common function. We wished to determine whether all functions of Abp1p require interaction with Srv2p or whether Abp1p performs any functions independent of Srv2p. If all functions of Abp1p involve binding to Srv2p, then mutations that specifically disrupt SH3 domain-mediated binding should phenotypically mimic null mutations in *ABP1*. To date, no readily assayed primary phenotypes have been described for *abp1* mutations, but one notable characteristic of *abp1* null mutations is "synthetic lethality" in combination with certain other mutations. Cells carrying mutations in the *SAC6*, *SLA1*, or *SLA2* genes are viable at 25°C, but any of these mutations in combination with an *abp1* null mutation is lethal (Holtzman *et al.*, 1993).

We first determined whether the Abp1p SH3 domain has a critical function in *ABP1*-dependent mutant backgrounds by examining the behaviors of *abp1* mutations targeted to the SH3 domain in strains carrying mutations in *SAC6*, *SLA1*, or *SLA2*. To accomplish this, we constructed strains which contain a mutation in one of these three genes as well as a null mutation in *ABP1* (Δ*abp1*). These *ABP1*-dependent strains are viable due to the presence of a wild-type copy of *ABP1* on a plasmid marked with the *URA3* auxotrophic marker gene. The above strains allowed us to test the function of *ABP1* mutants in a "plasmid shuffle" assay. In this assay, strains are transformed with the mutant *abp1* plasmids bearing the *HIS3* selectable marker, and grown on medium which selects for *HIS3* but not *URA3* function. Yeast cells containing a functional *HIS3*-marked version of *ABP1* will remain viable upon loss of the *URA3* marked plasmid, whereas those bearing a nonfunctional mutant do not. This can be monitored by assaying growth on medium containing 5-FOA, which selects against cells which harbor a wild-type *URA3* gene (Boeke *et al.*, 1987).

Plasmid-borne versions of *ABP1* in which the SH3 domain-coding sequence is deleted (pABP1Δ1) or is replaced by the cSrc SH3 domain (pABP1-Src) were constructed and tested for function in the plasmid shuffle assay. Figure 4 shows the results of this analysis. Neither of the above plasmids can functionally substitute for the wild-type *ABP1* gene, demonstrating that the Abp1p SH3 domain is required for the viability of *ABP1*-dependent strains. As an additional test of whether the specific loss of SH3 domain function can explain the behaviors of the above mutations, an additional Abp1p SH3 domain-targeted alteration was constructed.

The S7A14S SH3 is a chimeric domain comprised of cSrc SH3 domain amino acid sequences with the exception of those in positions 8–14 (Figure 4B), which are their Abp1p counterparts. Based on an extensive body of structural information for the cSrc and other SH3 domains, the substituted region is known to correspond to a highly variable specificity determining region of SH3 domains often referred to as the RT Src loop (Noble *et al.*, 1993). The S7A14S alteration is expected to result in a change in ligand specificity of the parent cSrc SH3 toward that of the Abp1p SH3 domain. The in vitro ligand specificity of the S7A14S domain demonstrated in Figure 4C shows that this is indeed the case (compare with Figure 3B), although some binding specificity for the cSrc SH3 ligand is retained.

The pS7A14S-encoded mutant protein contains just seven amino acids that differ from the protein produced by pABP1-Src, yet Figure 4A shows that the two plasmids behave very differently in the plasmid shuffle assay. The $abp1^{S7A14S}$ allele supports the viability of all three *ABP1*-dependent strains. The growth and morphologies of the Δ*abp1* strains carrying pS7A14S and the *sla1–7* or *sac6–102* mutations are indistinguishable from their counterparts carrying a wild-type copy of *ABP1* (pABP1$^+$) when restreaked onto rich medium, although the strain carrying the *sla2–5* mutation grows more slowly with pS7A14S than with pABP1$^+$. The $abp1^{S7A14S}$ allele is able to support the viability of an *sla1–7* strain equally well when chromosomally integrated or when on a plasmid, and the proteins produced by both the $abp1^{S7A14S}$ and $abp1^{Src}$

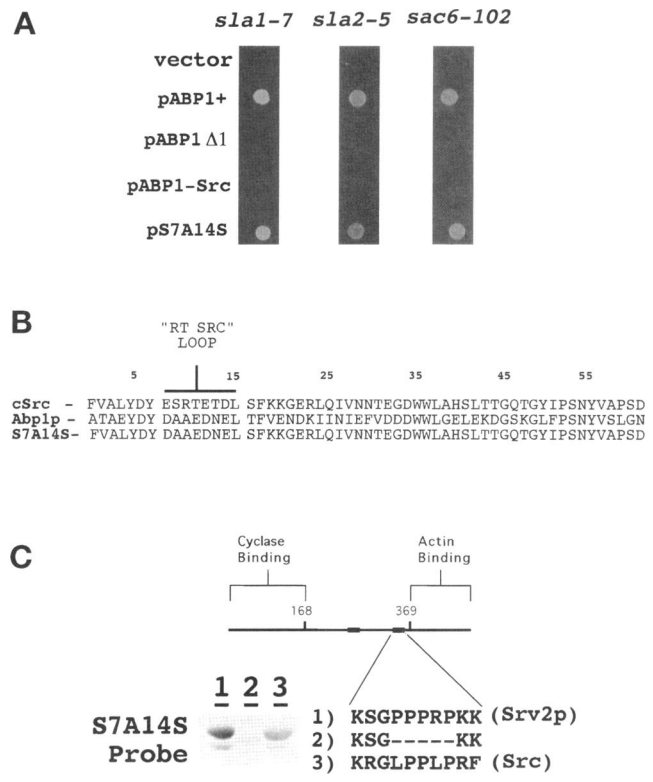

Figure 4. Effects of Abp1p SH3 domain-targeted mutations on Abp1p function and SH3 domain-binding specificity. (A) Plasmid shuffle assay demonstrating the capacity of plasmids carrying *ABP1* with SH3 domain alterations to function in genetic backgrounds requiring *ABP1* for viability. Strains DDY995 (left), DDY996 (middle), and DDY997 (right) harbor a chromosomal disruption of the *ABP1* gene as well as the indicated additional mutation conferring *ABP1* dependence. Strains originally carried a *URA3* marked plasmid containing a wild-type copy of *ABP1* (pDD13; Holtzman *et al.*). Strains were transformed with the indicated *HIS3* marked plasmids and for 4 d at 30°C on media selective for the *HIS3* but not the *URA3* marker. Transformants were then replica plated onto 5-FOA media to select against cells harboring the $HIS3^+$ $ABP1^+$ plasmid, and growth after 4 d at 30°C was photographed. (B) Alignment of chicken cSrc SH3 domain with Abp1p and mutant $abp1^{S7A14S}$ chimeric SH3 domains. Overline highlights RT Src loop region proposed to influence ligand specificity (Nobel *et al.*, 1993). (C) In vitro ligand specificity of S7A14S domain. Biotinylated GST fusion to the S7A14S SH3 domain (pGS7A14S) was used to probe purified GST fusions to: lane 1, Srv2p amino acds 337–376 (pGSRV2–1); lane 2, Srv2p amino acids 337–376 with amino acids 354–358 deleted (pGSRV2–2); and lane 3, Srv2p amino acids 337–376 with the SH3 domain-binding site residues at positions 352–360 altered to conform with the consensus for peptides which bind to the cSrc SH3 domain (pGSRV2–3). Plasmids used to direct expression of fusion proteins in *E. coli* appear in parentheses.

alleles colocalize with actin in a wild-type manner in double-label immunofluorescence experiments. Crude extracts from strains containing chromosomally integrated versions of the $abp1^{S7A14S}$ and $abp1^{Src}$ alleles yield equivalent signals in anti-Abp1p immunoblotting experiments, suggesting that the different behaviors of the two alleles do not stem from differences in steady-state expression levels.

Since only versions of *ABP1* having an SH3 domain with a binding specificity similar to the wild type are capable of supporting the viability of *ABP1*-dependent strains (Figure 4A), the results suggest that Abp1p SH3 domain ligand specificity is of central importance to Abp1p function in these genetic backgrounds. Because the Abp1p SH3 domain mediates the association of Srv2p with cortical actin patches, we expected that the ability of an *abp1* mutant allele to localize Srv2p to cortical patches would correlate with the capacity of the allele to function in the plasmid shuffle assay. Figure 5, however, shows that this is not the case. Although the $abp1^{S7A14S}$ allele functions almost as well as wild type in *ABP1*-dependent mutant backgrounds, Srv2p does not show obvious association with cortical actin patches in strains carrying this mutation. Srv2p is also delocalized in strains carrying the $abp1^{Src}$ allele.

The results of analysis of *ABP1* SH3-targeted mutations suggest that SH3 domain ligand specificity is a central aspect of the Abp1p function required in *sac6*, *sla1*, and *sla2* mutant backgrounds, but also suggest that this function is distinct from the function of Abp1p in mediating the cytoskeletal localization of Srv2p. These results are consistent with the possibility that the SH3 domain of Abp1p is capable of binding to a ligand in addition to Srv2p (see DISCUSSION). Even though all of the Abp1p mutant proteins we examined are capable of normal cortical actin patch localization, we cannot rule out the possibility that the failure of some *abp1* mutations to support the viability of *ABP1*-dependent strains is due to unintended effects of the mutations on functions of Abp1p which are not functions of the SH3 domain per se.

In any case, results of the analysis of the $abp1^{S7A14S}$ allele above suggest that a function of Abp1p required for viability in *ABP1*-dependent genetic backgrounds is separate from the function of Abp1p in mediating Srv2p subcellular localization. This predicts that *srv2* mutations which eliminate binding to the Abp1p SH3 domain should also have negligible effects on strains carrying mutations in *SLA1*, *SLA2*, or *SAC6*. We first determined whether wild-type Srv2p is required for the viability of *sla1*, *sla2*, or *sac6* mutants, or is required in strains carrying mutations in genes for other actin-associated proteins.

Figure 6 shows the results of tetrad analysis on strains doubly heterozygous for the *srv2*Δ2 disruption and marked gene disruptions in the *ABP1*, *SLA1*, *SLA2*, *RVS167*, and *SAC6* genes. Growth sufficient to produce visible colonies was not seen in segregants inferred to have *sla2/srv2* or *sac6/srv2* double mutant genotypes, establishing that Srv2p has a function which is essential for viability in strains carrying *sla2* or *sac6* mutations. In addition, an important function for Srv2p in *rvs167* mutant strains is demonstrated by

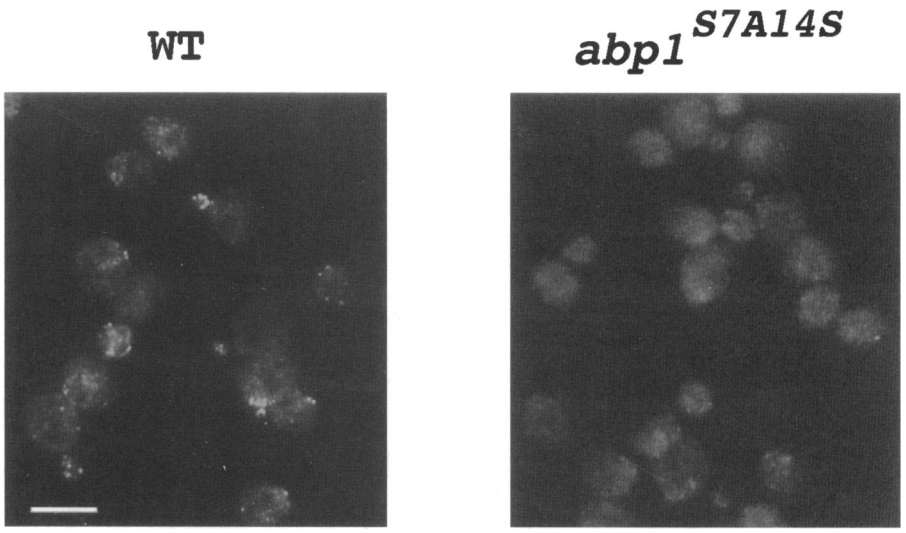

Figure 5. Effect of the *abp* ^{S7A14S} mutation on Srv2p immunofluorescence localization. Wild-type (WT) strain DDY998 (left) and isogenic strain DDY1103 (right), carrying a chromosomally integrated copy of the *abp1* ^{S7A14S} mutant allele containing a chimeric cSrc/Abp1p SH3 domain. Bar, 5 μm.

the fact that *rvs167/srv2* double mutant segregants form very small colonies relative to wild-type or to either single mutant strain. Combining null mutations in *SRV2* and *ABP1* does not result in negative synergism, and *sla1/srv2* double mutant strains are clearly viable as well.

The fact that *sla1/srv2* double mutant strains are viable while *sla1/abp1* double mutant strains are not implies that the essential function(s) of Abp1p in *sla1* mutant strains probably does not involve binding to Srv2p. An alternative formal possibility is that lethality of *sla1/abp1* double mutants is the result of deleterious effects of deregulated Srv2p. We rule out this possibility in the further observation that no viable *sla1/abp1/srv2* triple mutants could be obtained after sporulating a strain triply heterozygous for these gene disruptions.

To determine the effects of mutations that specifically affect the Srv2p SH3 domain-binding site in strains carrying mutations in *SLA2*, *SAC6*, and *RVS167*, we constructed strains which contain a mutation in one of these three genes as well as the *srv2*Δ*2* disruption. These *SRV2*-dependent strains are viable due to the presence of *SRV2*$^+$ on a plasmid and allowed us to test the function of a battery of *srv2* site-directed and deletion mutants in a plasmid shuffle assay similar to that shown in Figure 4A. The results of this analysis are shown in Figure 7. Plasmids pSRV2–2 and pSRV2–3, which contain the Abp1p SH3 domain-binding site mutations, are capable of supporting the viability of strains containing mutations in *RVS167*, *SAC6*, or *SLA2*. Strains harboring these plasmids are indistinguishable from their counterparts carrying wild-type *SRV2* (pSRV2–1) in terms of

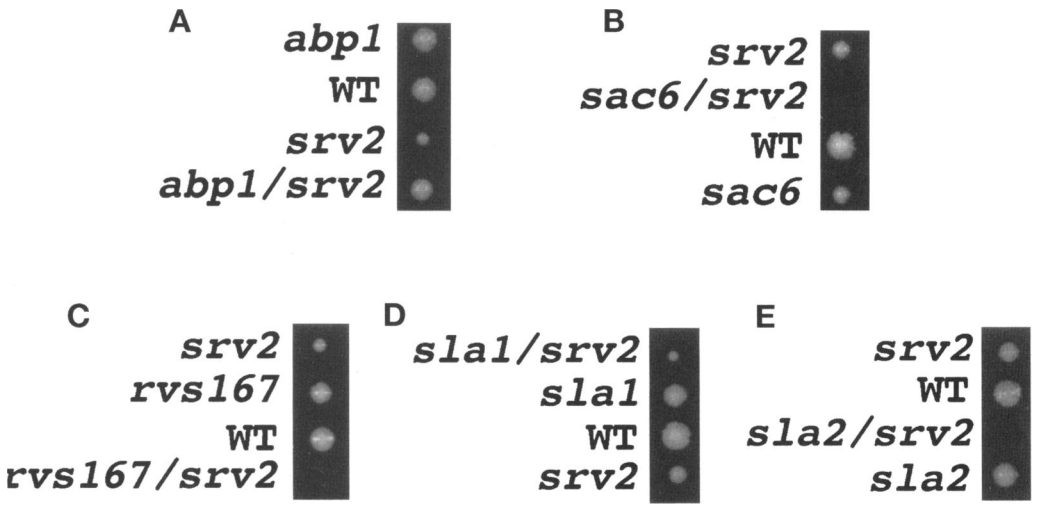

Figure 6. Effects of combining an *SRV2* null mutation with null mutations in genes encoding other actin-associated proteins. Growth of segregants of a representative tetratype ascus from strains doubly heterozygous for the *srv2*Δ*2* disruption and disruptions in other indicated genes is shown. Labels indicate which marked disruption mutations are inferred to be present based on segregation of auxotrophic markers. Parent strains are: A, DDY1010; B, DDY1011; C, DDY1014; D, DDY1012; and E, DDY1013. Photographs taken after 5 d of growth at 25°C (DDY1013) or 4 d of growth (others) at 30°C on YPD medium.

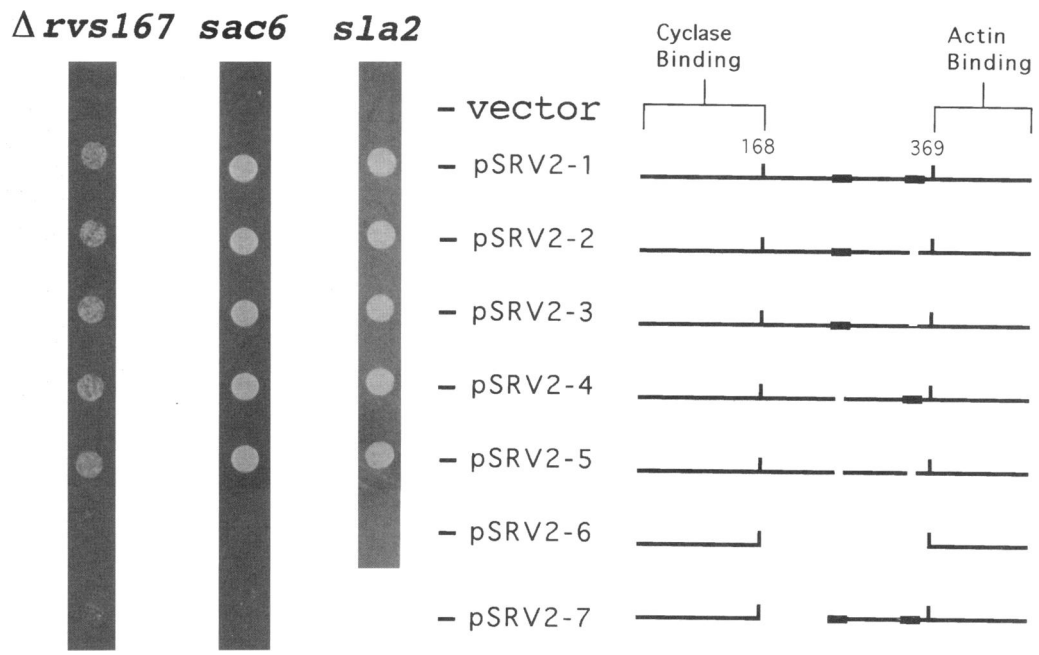

Figure 7. Effect of *SRV2* mutations on Srv2p function. Results of a plasmid shuffle assay demonstrating the capacity of *SRV2* deletion mutants to support the viability of strains dependent on *SRV2* for vegetative growth are shown. Schematic diagram of Srv2p domain structure and mutant versions tested appears at the right. Wide lines represent prominent proline-rich motifs corresponding to amino acids 267–285 and 354–358 of the Srv2p sequence. Thin line for pSRV2-3 represents mutation in the coding sequence for the Srv2p amino acid sequence (KSGPPPRPKK) to that of KRGLPPLPRF (see text for details). Strains DDY1021 (left), DDY1020 (middle), and DDY1019 (right) bear a chromosomal disruption in the *SRV2* gene and the additional mutation labeled that confers *SRV2* growth dependence. Each strain originally carried a wild-type copy of *SRV2* on a *URA3* marked plasmid (pDD210). Strains were transformed with the indicated *SRV2* derivative plasmids (marked with the *LEU2* gene) and grown for 5 d at 25°C on media selective for the *LEU2* but not the *URA3* marker. Strains were then replica plated onto 5-FOA medium to select against cells harboring the $URA3^+$ $SRV2^+$ plasmid, and growth after 4 d at 25°C was photographed.

growth rates and morphologies when grown in rich media after 5-fluoroorotic acid counterselection of the $URA3^+$ $SRV2^+$ plasmid. Thus, the binding site for the Abp1p SH3 domain in Srv2p is not required for the vegetative growth of any of the strains in which *SRV2* is essential. In addition, growth rates and morphologies of *sla1/srv2* double mutant strains transformed with either pSRV2–1, pSRV2–2, or pSRV2–3 are indistinguishable. It is unlikely that strong phenotypic effects (e.g., synthetic lethality) of the *srv2* mutations are being masked by selection for elevated plasmid copy number, since even significant overexpression of the *SRV2* gene from a strong constitutive promoter on a high copy number plasmid (pADH-CAP; Gerst *et al.* 1991) does not suppress the synthetic lethality of *abp1/sla1*, *abp1/sla2*, or *abp1/sac6* double mutant combinations in a plasmid shuffle assay.

In addition to the Abp1p SH3-binding site, Srv2p contains one prominent proline-rich amino acid motif spanning amino acids 267–285 which could conceivably function as a cryptic binding site for the Abp1p SH3 domain or as a binding site for another SH3 domain-containing protein. To test whether this region of Srv2p is required in *SRV2*-dependent strains, mutants were constructed which delete the coding sequences for amino acids 267–285 (pSRV2–4) or which delete this region in combination with deletion of coding sequences for the Abp1p SH3-binding site amino acids 354–358 (pSRV2–5). These *srv2* mutants are also capable of functioning in the place of wild-type *SRV2* in the plasmid shuffle assay (Figure 7). Further deletion analysis of *SRV2* identified larger regions of the gene which are required for viability of the *SRV2*-dependent strains, but plasmids carrying these *srv2* deletions (pSRV2–6, pSRV2–7; Figure 7) only partially rescue the slow growth and morphological defects of the *srv2*Δ2 disruption; therefore, it is unclear whether the inability of these plasmids to support the viability of *SRV2*-dependent strains is due to loss of a specific functional site in the Srv2 protein or is due to a general diminution of Srv2p function.

The above experiments show that *srv2* mutations which affect binding to the Abp1p SH3 domain cause no obvious phenotypic effects even in genetic backgrounds (*sac6*, *rvs167*, *sla1*, or *sla2*) in which *ABP1* and/or *SRV2* are required for viability. We conclude that the Srv2p-binding function of Abp1p is separate from another function(s) of Abp1p which is required for the viability of *ABP1*-dependent mutant strains. We also show that neither proline-rich region in Srv2p is required in *SRV2*-dependent genetic backgrounds. We conclude that the essential functions of Srv2p here are unlikely to involve binding by SH3 domain-containing proteins, and must reside in other regions of Srv2p such as the actin-binding or adenylyl cyclase-binding domains.

Mutations in RVS167 and ABP1 Show Similar Phenotypes and Genetic Interactions

Because the Rvs167p SH3 domain binds to a site in Abp1p in vitro (Figure 1), we wished to determine whether the functions of Rvs167p and Abp1p in vivo are closely related. As mentioned previously, *abp1* mutants do not display the obvious growth or morphological abnormalities associated with mutations in some other components of the actin cytoskeleton. *Abp1* mutant cells are indistinguishable from wild type for a number of properties which we and others have assessed, including growth rates and morphology at temperatures from 14 to 37°C (Drubin *et al.*, 1988), mating projection formation (Read *et al.*, 1992), and the kinetics of bud emergence after arrest of the cell cycle by mating pheromone or nutrient deprivation. Loss of function mutations in *RVS167* also have only subtle effects on cells growing in rich medium, but cause a number of phenotypes which are apparent in poor growth media. These include rapid loss of viability under starvation conditions or in medium containing sodium chloride, poor growth on media containing nonfermentable carbon sources, and failure of diploid mutant cells to undergo sporulation when starved (Bauer *et al.*, 1993; Desfarges *et al.*, 1993; Munn *et al.*, 1995).

To determine whether Abp1p and Rvs167p are likely to participate in related functions, we examined the behavior of *abp1* mutant strains in light of the known defects of *rvs167* mutants. The results presented in Table 2A show that Δ*abp1*/Δ*abp1* diploids undergo sporulation more than threefold less efficiently than their wild-type counterparts. This phenotype might result from perturbation of processes that involve either binding partner of Abp1p (Srv2p or Rvs167p). Srv2p has been implicated in adenylyl cyclase pathway signaling, and activation of this pathway, like the *RVS167* mutation, can result in reduced sporulation efficiency (reviewed in Broach and Deschenes, 1990; Broach, 1991). We show that the sporulation defect of Δ*abp1*/Δ*abp1* cells is not due to loss of the Srv2p-binding function of Abp1p, however, because *srv2*Δ*2*/*srv2*Δ*2* cells carrying a plasmid-borne wild-type copy of *SRV2* (pSRV2$^+$) sporulate with the same efficiency as cells carrying either a vector control plasmid or a plasmid containing the SH3 domain-binding site deletion mutant (pSRV2–2, Table 2B).

Phenotypes for Δ*abp1* haploid cells were also evident under some conditions in which similar defects have been observed in *rvs167* mutant cells. We compared the growth rates and viability of wild-type and Δ*abp1* mutant cells in media containing 5% sodium chloride (Figure 8A). When cells growing in rich medium were shifted to this medium at 37°C, an initial decrease in the number of viable Δ*abp1* mutant cells was observed. After a time, an increase in the number of viable Δ*abp1* mutant cells was observed, but the number remained significantly lower than the wild-type control. Similar results were obtained when viability of Δ*abp1* mutant cells transformed with a control vector or plasmid-borne *ABP1*$^+$ were compared, or when the viability of Δ*abp1* and wild-type cells grown in medium containing glycerol as a carbon source were compared. At time points when cells were increasing in number, we did not see evidence of multinucleate or anucleate cells in 4′,6-diamidino-2-phenylindole- stained samples, effects which might have been taken as evidence of defects in bud emergence or cytoskeletal checkpoint control (Lew and Reed, 1995). We speculate that the effect of *ABP1* mutation on cell viability may result from a loss of cortical integrity, since mutant cultures contained greater numbers of cells that appeared to have undergone lysis or that appeared darkened when viewed by phase-contrast microscopy. The growth rates and viability of *srv2*Δ*2* mutant cells containing either *SRV2*$^+$ on a plasmid (pSRV2–1) or *SRV2* missing the Abp1p SH3 domain-binding site (pSRV2–2) were indistinguishable when cells were grown in medium containing sodium chloride or glycerol, indicating that the effects of *abp1* mutation under these conditions are not due to loss of the Srv2p-binding function of Abp1p.

To further explore the possibility that Abp1p and Rvs167p function in concert, we determined whether Rvs167p is required for the phenotypic effects of Abp1p overexpression. Overexpression of *ABP1* from a high copy number plasmid in wild-type cells results in a poor cell growth coupled with abnormal cell morphology (Drubin *et al.*, 1988). Figure 8B shows that in *rvs167* null mutant cells, Abp1p overexpression has

Table 2. Sporulation efficiency—*abp1* and *srv2* mutant cells

Strain	Genotype	(plasmid)	% Sporulation	(SD)
	A. Δ*abp1* vs. wild type			
DDY1007	*ABP1*/*ABP1*		63.1	(3.2)
DDY1008	Δ*abp1*/Δ*abp1*		17.8	(2.0)
DDY1091	Δ*abp1*/Δ*abp1*	(pABP1+)[a]	66.5	
DDY1092	Δ*abp1*/Δ*abp1*	(vector)	24.4	
	B. *srv2* Mutant vs. wild type			
DDY1095	Δ*srv2*/Δ*srv2*	(pSRV2$^+$)	33.8	(0.7)
DDY1094	Δ*srv2*/Δ*srv2*	(vector)	34.7	
DDY1096	Δ*srv2*/Δ*srv2*	(pSRV2-2)	33.6	(4.6)

Sporulation was induced as described in MATERIALS AND METHODS, and the number of asci present after 14 d at 25°C was determined by phase-contrast microscopic examination. Approximately 300 cells were counted for each data point. Values shown for DDY1007 and DDY1008 are the average for three separate experimental trials, and values for DDY1095 and DDY1096 are the average of two trials. SD, standard deviation.

[a] Plasmids are indicated in parentheses.

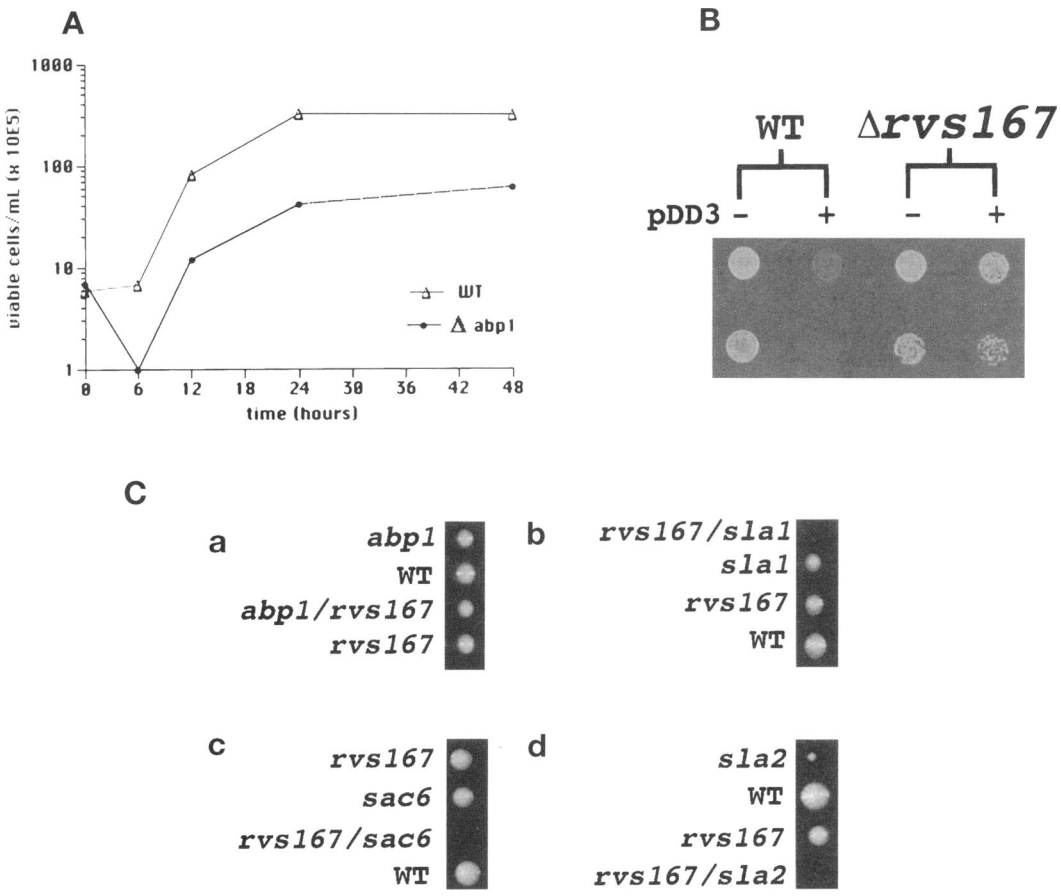

Figure 8. Phenotypic effects of ABP1 null mutations and Abp1p overexpression. (A) Viability of wild-type versus Δ*abp1* mutant cells in medium containing sodium chloride. Log phase cells of strain DDY898 (WT) or DDY321 (Δ*abp1*) were collected by centrifugation and transferred to SD medium containing 5% sodium chloride. At time points, aliquots were plated for viability as described in MATERIALS AND METHODS. (B) Effect of Abp1p overexpression in wild-type and Δ*rvs167* strains. Wild-type strain DDY78 or Δ*rvs167* strain DDY950 was transformed with a control vector plasmid (−) or a high copy number plasmid carrying the *ABP1* gene (+, pDD3). Approximately 10^5 (top) or 10^4 (bottom) transformed cells suspended in water were spotted onto medium selective for the plasmid auxotrophic marker and photographed after 72 h of growth at 34°C. (C) Effect of *RVS167* null mutation on growth of strains carrying mutations in *ABP1* or in other genes which confer *ABP1* dependence. Growth of segregants of a representative tetratype ascus from strains doubly heterozygous for an *RVS167* gene disruption and disruptions in other indicated genes is shown. Labels indicate which marked disruption mutations are inferred to be present on segregation of auxotrophic markers. WT, wild type. Parent strains are: a, DDY991; b, DDY992; c, DDY993; and d, DDY994.

a less deleterious effect on growth than in wild-type cells. This observation is consistent with the possibility that an Abp1p/Rvs167p complex is the agent of the deleterious effect of *ABP1* overexpression. *ABP1* overexpression is more detrimental to cell growth than loss of the *RVS167* gene; therefore, the effects of *ABP1* overexpression in otherwise wild-type cells cannot be solely caused by simple sequestration of Rvs167p. Deleterious effects of a complex which includes both Abp1p and Rvs167p might result from the mislocalization of the complex, or may be due to sequestration of other cellular components which bind to Abp1p/Rvs167p complexes.

As an additional test of the relatedness of Abp1p and Rvs167p function, we determined whether an *rvs167* null mutation is synthetically lethal in combination with disruptions of the *ABP1*, *SLA1*, *SLA2*, and *SAC6* genes. Figure 8C shows that unlike null mutations in *SRV2* or any other cytoskeletal gene tested to date, the Δ*rvs167* mutation is synthetically lethal in combination with disruptions of all three of the genes that display synthetic lethality in combination with *abp1* mutations. The Δ*rvs167* mutation does not display negative growth synergism in combination with the Δ*abp1* disruption itself. These observations are consistent with a model in which Rvs167p and Abp1p participate in a common function that is dispensable under standard growth conditions but is essential for viability when *sla1*, *sla2*, or *sac6* mutations are present.

DISCUSSION

Even in a relatively simple cell type such as budding yeast, the functioning of the actin cytoskeleton is mechanistically complex, requiring coordination of the activities of many proteins. The complex yet specific network of interactions among mutations in the genes encoding actin-associated proteins (Figure 9A) suggests that the activities of proteins in the cortical patch structures are highly integrated. A thorough understanding of the domain structures, physical interactions, and subcellular localizations of actin-asso-

ciated proteins, as well as thorough genetic characterizations of mutations in the genes encoding them may all be required to illuminate the specific molecular processes which occur at the actin patch sites.

The work presented here furthers understanding of the physical and functional interactions of Abp1p with other actin-associated proteins (Figure 9B). Abp1p is capable of binding to Srv2p via its SH3 domain and can also associate with Rvs167p by virtue of a site in Abp1p that is bound by the Rvs167p SH3 domain (Figure 1; Freeman *et al.*, 1996). Phenotypic analysis of mutations that affect Abp1p, Rvs167p, and Srv2p shows that all three proteins function in cellular responses to adverse or changing environmental conditions, but also provides insight into the nature of the unique contribution that each protein makes to the integrated functioning of the actin cytoskeleton.

Comparison of phenotypes associated with *abp1* and *rvs167* mutations strongly suggests that the functions of the two proteins are closely related. *Abp1* mutant defects in sporulation and cell viability in poor growth media are similar to, although milder than, defects reported for *rvs167* mutations (Figure 8A; Table 2). *Abp1* and *rvs167* null mutations show similar profiles of genetic synthetic-lethal interactions with genes encoding components of the cortical cytoskeleton (Figure 8C), and the deleterious effects of Abp1p overexpression are ameliorated by deletion of *RVS167* (Figure 8B). These observations are consistent with a model in which binding to Abp1p modifies the activity of Rvs167p, perhaps by influencing the subcellular localization of Rvs167p or by influencing the association of Rvs167p with actin and/or other cellular factors.

Rvs167p shows sequence similarity with human amphiphysin (David *et al.*, 1994; Sivadon *et al.*, 1995). Amphiphysin has been proposed to function in endocytosis of synaptic vesicles, and mutations in *RVS167* have been shown to affect fluid phase endocytosis in yeast (Munn *et al.*, 1995). The SH3 domain of amphiphysin has been shown to be capable of binding to dynamin and to synaptojanin, two proteins also thought to play roles in synaptic vesicle recycling (David *et al.*, 1996; McPherson *et al.*, 1996). By analogy, the Rvs167p SH3 domain might also bind to ligands having functions in endocytosis. The yeast dynamin homologues Vps1p/Spo15p and Dnm1p do not contain sequence motifs similar to known SH3 domain-binding sites (Yeh *et al.*, 1991; Gammie *et al.*, 1995), however, suggesting that they do not physically interact with the Rvs167p SH3 domain. One possibility then is that Abp1p has a function in endocytosis. *ABP1* mutation does not dramatically affect the uptake of extracellular α factor (Kubler and Riezman, 1993); therefore, Abp1p may have a subtle role in this process.

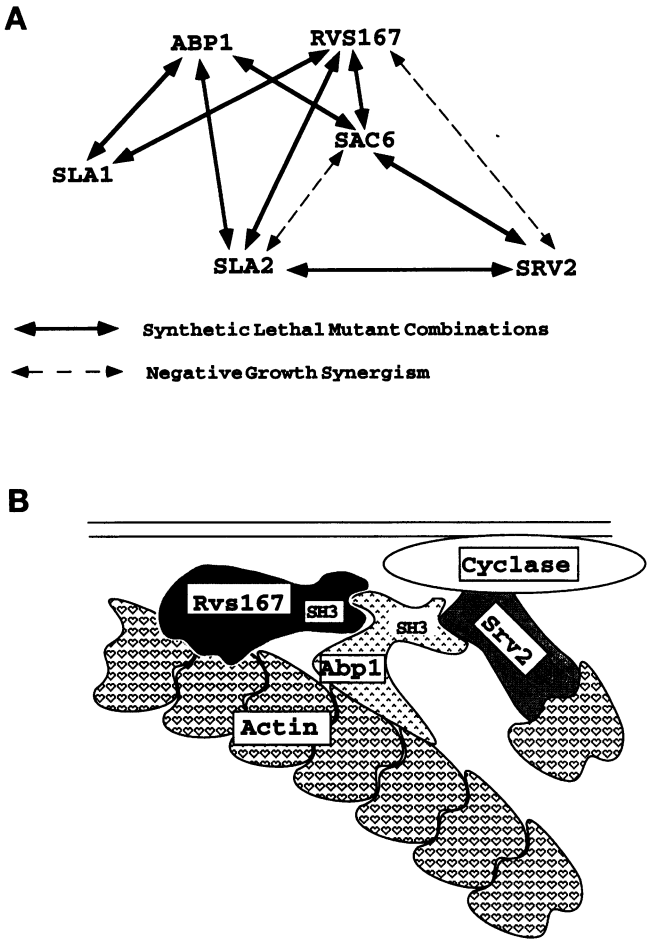

Figure 9. Genetic and physical interactions among *S. cerevisiae* actin-associated proteins. (A) Summary of lethal double mutant combinations among disruptions in the *ABP1*, *RVS167*, *SAC6*, *SLA1*, *SLA2*, and *SRV2* genes. (B) Hypothetical cortical protein complex based on demonstrated binding interactions. Thin double line at the top represents the plasma membrane. Interaction of actin and Rvs167p is based on two-hybrid data (Amberg *et al.*, 1995). Direct binding of the two proteins has not been demonstrated, and it is not known whether monomeric or filamentous actin is the relevant binding partner.

An N-terminal 180- amino acid fragment of Abp1p binds to filamentous actin in vitro (Chamany and Drubin, unpublished results) and has sequence similarity to proteins of the ADF/cofilin family (reviewed in Moon and Drubin, 1995), *Dictyostelium* coactosin (de Hostos *et al.*, 1993), and an N-terminal domain of the vertebrate neuronal actin-binding protein drebrin (23% amino acid identity with rat drebrin A over a 130-amino acid span; see MATERIALS AND METHODS). Cofilins can sever actin filaments while coactosin and drebrin do not; therefore, these evolutionarily related proteins clearly do not all function in a precisely analogous manner, but a common theme may lie in the roles of these proteins as stimulus-responsive

modulators of actin filament architecture and dynamics. A large body of evidence links changes in the activity of cofilin, for example, to cytoskeletal rearrangements which occur in response to receptor stimulation in cells such as platelets and T-cells (Moon and Drubin, 1995). Marked changes in the association of drebrin with cellular actin-containing structures accompanies the retinoic acid-induced differentiation of neuroblastoma cells (Asada *et al.*, 1994), and expression of drebrin in non-neuronal cell types leads to the formation of neurite-like outgrowths (Shirao *et al.*, 1992). Like cofilin and drebrin, Abp1p may exert effects on actin filament architecture in response to stimulation of signal transduction pathways by extracellular cues. This possibility is consistent with the *abp1* mutant phenotypes reported here and with evidence for the indirect association of Abp1p with adenylyl cyclase via Srv2p (see below).

Srv2p immunolocalization experiments provide strong evidence that the Abp1p SH3 domain mediates the association of Srv2p with cortical actin patches in vivo (Figures 2, 3C, and 6). Although our experiments cannot distinguish whether Srv2p in *abp1* mutant cells actually fails to associate with cortical actin patches in living cells or is not associated stably enough to withstand the cell fixation and staining protocol, the apparent loss of Srv2p cortical patch association is a specific effect of *abp1* mutations or mutations in the Srv2p-binding site for the Abp1p SH3 domain. We conclude that the normal localization and/or stable association of Srv2p with cortical actin patch structures requires Abp1p. Thorough comparison of phenotypes associated with mutations in *ABP1* and *SRV2*, however, shows that the Srv2p-binding function of Abp1p is not required for any of the previously known or newly discovered genetically defined functions of *ABP1* (Figures 4–7). We also identify genetic backgrounds in which Srv2p is essential for viability (Figure 6) and show that neither of the proposed SH3 domain-binding sites in Srv2p (Freeman *et al.*, 1996) are required in those backgrounds (Figure 7). Srv2p homologues in other species, like yeast Srv2p, associate with cortical actin-containing structures (Vojtek and Cooper, 1993; Gottwald *et al.*, 1996), but at the present time we can only speculate as to what the precise function of this association may be.

Srv2p binds to adenylyl cyclase in vivo and has a role in generating the abnormally high intracellular cAMP levels associated with mutational activation of Ras2p. However, its role in normal RAS/adenylyl cyclase pathway signaling has yet to be elucidated (Fedor-Chaiken *et al.*, 1990; Wang *et al.*, 1992, 1993). cAMP-dependent protein kinase-mediated signals are required for growth and cell cycle progression past the unbudded (G_1) stage in *S. cerevisiae*, and recent reports have suggested that cAMP-mediated events can also delay the timing of bud emergence by exerting a negative effect on G_1 cyclin synthesis (Broach, 1991; Baroni *et al.*, 1994; Tokiwa *et al.*, 1994). Although changes in actin organization which underlie bud emergence are controlled by changes in cyclin-dependent kinase activity (Lew and Reed, 1993), it is also possible that the Ras proteins and downstream effectors provide additional regulatory inputs into the cytoskeletal and/or secretory functions responsible for cell surface growth. In nerve synaptic termini, changes in the phosphorylation states of vesicle-associated proteins have been proposed to regulate a number of processes required for neurotransmitter exocytosis, including dissociation of vesicles from the actin cytoskeleton, vesicle-plasma membrane docking, and vesicle-plasma membrane fusion (reviewed in Greengard *et al.*, 1993). One possibility in budding yeast is that Abp1p and Srv2p, through interaction with adenylyl cyclase, affect the local activity of cAMP-dependent protein kinases and thus assist in the regulation of functionally similar phosphorylation events that influence vesicle delivery or fusion at the bud site. A role for Srv2p in influencing secretory processes is consistent with the observation that overexpression of *SNC1*, which encodes a homologue of the synaptic vesicle-associated protein synaptobrevin, partially suppresses defects associated with an *srv2* mutation (Gerst *et al.*, 1992).

Although our results demonstrate that binding of the Abp1p SH3 domain to Srv2p is not required for the viability of *ABP1*-dependent strains (Figure 7), an Abp1p SH3 domain having a ligand specificity similar to wild type is apparently required in these backgrounds. Since all functional versions of Abp1p contain SH3 domains capable of binding to the Srv2p sequence KSGPPPRPKK (Figures 3B, 4A, and 4C), one possibility is that the Abp1p SH3 domain binds to a ligand in addition to Srv2p containing a similar sequence. Candidates include a protein implicated in bipolar bud site selection, Bud8p (Zahner *et al.*, 1996), predicted to contain the sequence KNGTPPRPTS (GenBank accession number L37016), and a hypothetical ankyrin repeat-containing protein containing the sequence KTTPPPAPRS (GenBank accession number L28920). The possibility that Abp1p binds to Bud8p is intriguing in light of the fact that Abp1p overproduction causes haploid cells, which normally bud in an axial pattern, to adopt the bipolar budding pattern characteristic of diploids.

In our examination of the phenotypes of a new *srv2* deletion mutant, we find one significant difference from previous characterizations. The *srv2*Δ*2* mutation does not result in inviability on rich media (Figure 3A). Our motivation for generating a new *srv2* deletion allele stemmed from the curious behavior of the preexisting deletion under certain conditions we examined. Either in the original strain background or when outcrossed to the SC288 background four times,

strains carrying the *srv2* deletion, but also carrying any of several independently isolated genomic DNA fragments carrying *SRV2*$^+$ on a plasmid, were unable to grow on glycerol-containing medium. Strains carrying the *srv2*Δ*2* mutation and one of the *SRV2*$^+$ plasmids grow as well as the wild type on this medium. We speculate that the strain isolate carrying the original deletion that we used may carry an additional mutation in a gene linked to *SRV2*, or that the effect described may be due to expression of a small N-terminal region of Srv2p which is left intact by the deletion.

Despite the fact that *ABP1* is dispensable for the growth of yeast in the laboratory, work presented here demonstrates that it participates in a complex set of interactions which become important for cell survival when environmental stresses are introduced. Evidence for the physical and functional association of Abp1p with Rvs167p and Srv2p suggests that endocytosis, actin assembly, and adenylyl cyclase signaling are coordinated to maximize cell fitness and adaptability.

ACKNOWLEDGMENTS

We thank Jasper Rine, Kathryn Ayscough, Fred Chang, Jamie Cope, and Marc Rose for helpful discussions. We thank Alan Bender, Jeffrey Field, Nancy Freeman, and Michele Aigle for providing strains and plasmids. This work was supported by grants to D.D. from the National Institutes of General Medical Sciences (GM-42759) and the American Cancer Society (CB-106 and FRA-442).

REFERENCES

Adams, A.E., Botstein, D., and Drubin, D.G. (1989). A yeast actin-binding protein is encoded by *SAC6*, a gene found by suppression of an actin mutation. Science *243*, 231–233.

Altschul, S.F., Gish, W., Miller, W., Myers, E.W., and Lipman, D.J. (1990). Basic local alignment search tool. J. Mol. Biol. *215*, 403–410.

Amberg, D., Basart, E., and Botstein, D. (1995). Defining protein interactions with yeast actin in vivo. Nat. Struct. Biol. *2*, 28–35.

Asada, H., Uyemura, K., and Shirao, T. (1994). Actin-binding protein, drebrin, accumulates in submembranous regions in parallel with neuronal differentiation. J. Neurosci. Res. *38*, 149–159.

Ausubel, F. (1990). Expression and purification of glutathione-S-transferase fusion proteins. In: Current Protocols in Molecular Biology, ed. F. Ausubel, New York: Greene Publishing Associates and Wiley-Interscience.

Ayscough, K.A., and Drubin, D.G. (1996). Actin: general principles from studies in yeast. Annu. Rev. Cell Dev. Biol. *12*, 129–160.

Baroni, M., Monti, P., and Alberghina, L. (1994). Repression of growth-regulated G_1 cyclin expression by cyclic AMP in budding yeast. Nature *371*, 339–342.

Baudin, A., Ozier, K.O., Denouel, A., Lacroute, F., and Cullin, C. (1993). A simple and efficient method for direct gene deletion in *Saccharomyces cerevisiae*. Nucleic Acids Res. *21*, 3329–3330.

Bauer, F., Urdaci, M., Aigle, M., and Crouzet, M. (1993). Alteration of a yeast SH3 protein leads to conditional viability with defects in cytoskeletal and budding patterns. Mol. Cell. Biol. *13*, 5070–5084.

Bement, W.M., Wirth, J.A., and Mooseker, M.S. (1994). Cloning and mRNA expression of human unconventional myosin-IC. A homologue of amoeboid myosins-I with a single IQ motif and an SH3 domain. J. Mol. Biol. *243*, 356–363.

Bender, L., Lo, H., Lee, H., Kokojan, V., Peterson, J., and Bender, A. (1996). Associations among PH and SH3 domain-containing proteins and Rho-type GTPases in yeast. J. Cell Biol. *133*, 879–894.

Boeke, J.D., Trueheart, J., Natsoulis, G., and Fink, G.R. (1987). 5-Fluoro-orotic acid as a selective agent in yeast molecular genetics. Methods Enzymol. *154*, 164–175.

Broach, J.R. (1991). Ras-related signaling processes in *Saccharomyces cerevisiae*. Curr. Opin. Gen. Dev. *1*, 370–377.

Broach, J.R., and Deschenes, R.J. (1990). The function of Ras genes in *Saccharomyces cerevisiae*. Adv. Cancer Res. *54*, 79–139.

Chenevert, J., Corrado, K., Bender, A., Pringle, J., and Herskowitz, I. (1992). A yeast gene (*BEM1*) necessary for cell polarization whose product contains two SH3 domains. Nature *356*, 77–79.

Cicchetti, P., Mayer, B.J., Thiel, G., and Baltimore, D. (1992). Identification of a protein that binds to the SH3 region of Abl and is similar to Bcr and GAP-rho. Science *257*, 803–806.

David, C., McPherson, P., Mundigl, O., and De Camilli, P. (1996). A role of amphiphysin in synaptic vesicle endocytosis is suggested by its binding to dynamin in nerve terminals. Proc. Natl. Acad. Sci. USA *93*, 331–335.

David, C., Solimena, M., and De Camilli, P. (1994). Autoimmunity in Stiff-man syndrome with breast cancer is targeted to the C-terminal region of human amphiphysin, a protein similar to the yeast proteins, Rvs167 and Rvs161. FEBS Lett. *351*, 73–79.

de Hostos, E.L., Bradtke, B., Lottspeich, F., and Gerisch, G. (1993). Coactosin, a 17 kDa F-actin binding protein from *Dictyostelium discoideum*. Cell Motil. Cytoskeleton *26*, 181–191.

Desfarges, L., Durrens, P., Juguelin, H., Cassagne, C., Bonneu, M., and Aigle, M. (1993). Yeast mutants affected in viability upon starvation have a modified phospholipid composition. Yeast *9*, 267–277.

Drubin, D.G., Miller, K.G., and Botstein, D. (1988). Yeast actin-binding proteins: evidence for a role in morphogenesis. J. Cell Biol. *107*, 2551–2561.

Drubin, D.G., Mulholland, J., Zhimin, Z., and Botstein, D. (1990). Homology of a yeast actin-binding protein to signal transduction proteins and myosin-I. Nature *343*, 288–290.

Drubin, D.G., and Nelson, W.J. (1996). Origins of cell polarity. Cell *84*, 335–344.

Fedor-Chaiken, M., Deschenes, R.J., and Broach, J.R. (1990). SRV2, a gene required for *RAS* activation of adenylate cyclase in yeast. Cell *61*, 329–340.

Field, J., *et al.* (1990). Cloning and characterization of CAP, the *S. cerevisiae* gene encoding the 70 kd adenylyl cyclase-associated protein. Cell *61*, 319–327.

Flynn, D.C., Leu, T.H., Reynolds, A.B., and Parsons, J.T. (1993). Identification and sequence analysis of cDNAs encoding a 110-kilodalton actin filament-associated pp60src substrate. Mol. Cell. Biol. *13*, 7892–7900.

Freeman, N.L., Chen, Z., Horenstein, J., Weber, A., and Field, J. (1995). An actin monomer binding activity localizes to the carboxyl-terminal half of the *Saccharomyces cerevisiae* cyclase-associated protein. J. Biol. Chem. *270*, 5680–5685.

Freeman, N.L., Lila, T., Mintzer, K.A., Chen, Z., Pahk, A.J., Ren, R., Drubin, D.G., and Field, J. (1996). A conserved proline-rich region of the *Saccharomyces cerevisiae* cyclase-associated protein binds SH3 domains and modulates cytoskeletal localization. Mol. Cell. Biol. *16*, 548–556.

Gammie, A.E., Kurihara, L.J., Vallee, R.B., and Rose, M.D. (1995). DNM1, a dynamin-related gene, participates in endosomal trafficking in yeast. J. Cell Biol. *130*, 553–566.

Gerst, J., Fergusen, K., Vojtek, A., Wigler, M., and Field, J. (1991). CAP is a bifunctional component of the *Saccharomyces cerevisiae* adenylyl cyclase complex. Mol. Cell. Biol. *11*, 1248–1257.

Gerst, J.E., Rodgers, L., Riggs, M., and Wigler, M. (1992). SNC1, a yeast homolog of the synaptic vesicle-associated membrane protein/synaptobrevin gene family: genetic interactions with the *RAS* and *CAP* genes. Proc. Natl. Acad. Sci. USA *89*, 4338–4342.

Gieselmann, R., and Mann, K. (1992). ASP-56, a new actin sequestering protein from pig platelets with homology to CAP, an adenylate cyclase-associated protein from yeast. FEBS Lett. *298*, 149–153.

Goodson, H.V., Anderson, B.L., Warrick, H.M., Pon, L.A., and Spudich, J.A. (1996). Synthetic lethality screen identifies a novel yeast myosin I gene (*MYO5*): myosin I proteins are required for polarization of the actin cytoskeleton. J. Cell Biol. *133*, 1277–1291.

Gottwald, U., Brokamp, R., Karakesisoglou, I., Schleicher, M., and Noegel, A.A. (1996). Identification of a cyclase-associated protein (CAP) homologue in *Dictyostelium discoideum* and characterization of its interaction with actin. Mol. Biol. Cell *7*, 261–272.

Greengard, P., Valtorta, F., Czernik, A.J., and Benfenati, F. (1993). Synaptic vesicle phosphoproteins and regulation of synaptic function. Science *259*, 780–785.

Gumbiner, B.M. (1996). Cell adhesion: the molecular basis of tissue architecture and morphogenesis. Cell *84*, 345–357.

Harlow, E., and Lane, D. (1988a). Immunoaffinity purification. In: Antibodies—A Laboratory Manual, ed. H.J. Cuddihy. Cold Spring Harbor, NY: Cold Spring Harbor Laboratory Press, 511–552.

Harlow, E., and Lane, D. (1988b). Immunoblotting. In: Antibodies—A Laboratory Manual, H.J. Cuddihy. Cold Spring Harbor, NY: Cold Spring Harbor Laboratory Press, 471–504.

Hildebrand, J.D., Taylor, J.M., and Parsons, J.T. (1996). An SH3 domain-containing GTPase-activating protein for Rho and Cdc42 associates with focal adhesion kinase. Mol. Cell. Biol. *16*, 3169–3178.

Holtzman, D.A., Yang, S., and Drubin, D.G. (1993). Synthetic-lethal interactions identify two novel genes, *SLA1* and *SLA2*, that control membrane cytoskeleton assembly in *Saccharomyces cerevisiae*. J. Cell Biol. *122*, 635–644.

Innis, M.A., Gelfand, D.H., Sninsky, J.J., and White, T.J. (1990). PCR Protocols, San Diego, CA: Academic Press.

Ito, H., Fukuda, Y., Murata, K., and Kimura, A. (1983). Transformation of intact yeast cells treated with alkali cations. J. Bacteriol. *153*, 163–168.

Kubler, E., and Riezman, H. (1993). Actin and fimbrin are required for the internalization step of endocytosis in yeast. EMBO J. *12*, 2855–2862.

Lauffenburger, D.A., and Horwitz, A. (1996). Cell migration: a physically integrated molecular process. Cell *84*, 359–369.

Lew, D.J., and Reed, S.I. (1993). Morphogenesis in the yeast cell cycle: regulation by Cdc28 and cyclins. J. Cell Biol. *120*, 1305–1320.

Lew, D.J., and Reed, S.I. (1995). A cell cycle checkpoint monitors cell morphogenesis in budding yeast. J. Cell Biol. *129*, 739–749.

Matsui, Y., Matsui, R., Akada, R., and Toh-e, A. (1996). Yeast src homology region 3 domain-binding proteins involved in bud formation. J. Cell Biol. *133*, 865–878.

Mayer, B.J., and Eck, M.J. (1995). Minding your p's and q's. Curr. Biol. *5*, 364–367.

McPherson, P.S., Garcia, E.P., Slepnev, V.I., David, C., Zhang, X., Grabs, D., Sossin, W.S., Bauerfeind, R., Nemoto, Y., and De, C.P. (1996). A presynaptic inositol-5-phosphatase. Nature *379*, 353–357.

Merilainen, J., Palovuori, R., Sormunen, R., Wasenius, V.M., and Lehto, V.P. (1993). Binding of the alpha-fodrin SH3 domain to the leading lamellae of locomoting chicken fibroblasts. J. Cell Sci. *105*, 647–654.

Mintzer, K.A., and Field, J. (1994). Interactions between adenylyl cyclase, CAP and RAS from *Saccharomyces cerevisiae*. Cell Signal *6*, 681–694.

Mitchison, T.J., and Cramer, L.P. (1996). Actin-based cell motility and cell locomotion. Cell *84*, 371–379.

Moon, A., and Drubin, D.G. (1995). The ADF/cofilin proteins: stimulus-responsive modulators of actin dynamics. Mol. Biol. Cell *6*, 1423–1431.

Munn, A.L., Stevenson, B.J., Geli, M.I., and Riezman, H. (1995). *end5*, *end6*, and *end7*: mutations that cause actin delocalization and block the internalization step of endocytosis in *Saccharomyces cerevisiae*. Mol. Biol. Cell *6*, 1721–1742.

Noble, M., Musacchio, A., Saraste, M., Courtneidge, S., and Wierenga, R. (1993). Crystal structure of the SH3 domain in human Fyn; comparison of the three-dimensional structures of SH3 domains in tyrosine kinases and spectrin. EMBO J. *12*, 2617–2624.

Noegel, A.A., and Luna, J.E. (1995). The *Dictyostelium* cytoskeleton. Experientia, *51*, 1135–1143.

Pearson, W.R., and Lipman, D.J. (1988). Improved tools for biological sequence comparison. Proc. Natl. Acad. Sci. USA *85*, 2444–2448.

Pollard, T.D., and Cooper, J.A. (1986). Actin and actin binding proteins. A critical evaluation of mechanisms and functions. Annu. Rev. Biochem. *55*, 987–1035.

Pringle, J.R., Adams, A.E., Drubin, D.G., and Haarer, B.K. (1991). Immunofluorescence methods for yeast. Methods Enzymol. *194*, 565–602.

Pringle, J.R., Preston, R.A., Adams, A.E., Stearns, T., Drubin, D.G., Haarer, B.K., and Jones, E.W. (1989). Fluorescence microscopy methods for yeast. Methods Cell Biol. *31*, 357–435.

Read, E.B., Okamura, H.H., and Drubin, D.G. (1992). Actin- and tubulin-dependent functions during *Saccharomyces cerevisiae* mating projection formation. Mol. Biol. Cell *3*, 429–444.

Rose, M.D., Novick, P., Thomas, J.H., Botstein, D., and Fink, G.R. (1987). A *Saccharomyces cerevisiae* genomic plasmid bank based on a centromere-containing shuttle vector. Gene *60*, 237–243.

Rose, M.D., Winston, F., and Hieter, P. (1990). Methods in Yeast Genetics, Cold Spring Harbor, NY: Cold Spring Harbor Laboratory Press.

Sambrook, J., Fritsch, E.F., and Maniatis, T. (1989). Molecular Cloning, A Laboratory Manual, Cold Spring Harbor, NY: Cold Spring Harbor Laboratory Press.

Shirao, T., Kojima, N., and Obata, K. (1992). Cloning of drebrin A and induction of neurite-like processes in drebrin-transfected cells (published erratum appears in Neuroreport *3*, 1992, following 285). Neuroreport *3*, 109–112.

Sikorski, R.S., and Hieter, P. (1989). A system of shuttle vectors and yeast host strains designed for efficient manipulation of DNA in *Saccharomyces cerevisiae*. Genetics *122*, 19–27.

Sivadon, P., Bauer, F., Aigle, M., and Crouzet, M. (1995). Actin cytoskeleton and budding pattern are altered in the yeast *rvs161* mutant: the Rvs161 protein shares common domains with the brain protein amphiphysin. Mol. Gen. Genet. *246*, 485–495.

Stoffler, H.E., Ruppert, C., Reinhard, J., and Bahler, M. (1995). A novel mammalian myosin I from rat with an SH3 domain localizes

to Con A-inducible, F-actin-rich structures at cell-cell contacts. J. Cell Biol. *129*, 819–830.

Stossel, T.P., *et al.* (1985). Nonmuscle actin binding proteins. Annu. Rev. Cell Biol. *1*, 353–402.

Sullivan, W., and Therkauf, W.E. (1995). The cytoskeleton and morphogenesis of the early *Drosophila* embryo. Curr. Opin. Cell Biol. *7*, 18–22.

Sun, H.Q., Kwiatkowska, K., and Yin, H.L. (1995). Actin monomer binding proteins. Curr. Opin. Cell Biol. *7*, 102–110.

Tokiwa, G., Tyers, M., Volpe, T., and Futcher, B. (1994). Inhibition of G_1 cyclin activity by the Ras/cAMP pathway in yeast. Nature *371*, 342–345.

Turner, C.E., and Miller, J.T. (1994). Primary sequence of paxillin contains putative SH2 and SH3 domain binding motifs and multiple LIM domains: identification of a vinculin and pp125Fak-binding region. J. Cell Sci. *107*, 1583–1591.

Vojtek, A.B., and Cooper, J.A. (1993). Identification and characterization of a cDNA encoding mouse CAP: a homolog of the yeast adenylyl cyclase associated protein. J. Cell Sci. *105*, 777–785.

Wang, J., Suzuki, N., and Kataoka, T. (1992). The 70-kilodalton adenylyl cyclase-associated protein is not essential for interaction of *Saccharomyces cerevisiae* adenylyl cyclase with *RAS* proteins. Mol. Cell. Biol. *12*, 4937–4945.

Wang, J., Suzuki, N., Nishida, Y., and Kataoka, T. (1993). Analysis of the function of the 70-kilodalton cyclase-associated protein (CAP) by using mutants of yeast adenylyl cyclase defective in CAP binding. Mol. Cell. Biol. *13*, 4087–4097.

Wang, K., Knipfer, M., Huang, Q.Q., van Heerden, A., Hsu, L.C., Gutierrez, G., Quian, X.L., and Stedman, H. (1996). Human skeletal muscle nebulin sequence encodes a blueprint for thin filament architecture. Sequence motifs and affinity profiles of tandem repeats and terminal SH3. J. Biol. Chem. *271*, 4304–4314.

Welch, M.D., Holtzman, D.A., and Drubin, D.G. (1994). The yeast actin cytoskeleton. Curr. Opin. Cell Biol. *6*, 110–119.

Wu, H., and Parsons, J.T. (1993). Cortactin, an 80/85-kilodalton Pp 60src substrate, is a filamentous actin-binding protein enriched in the cell cortex. J. Cell Biol. *120*, 1417–1426.

Yeh, E., Driscoll, R., Coltrera, M., Olins, A., and Bloom, K. (1991). A dynamin-like protein encoded by the yeast sporulation gene SPO15. Nature *349*, 713–715.

Yu, H., Chen, J., Feng, S., Dalgarno, D., Brauer, A., and Schreiber, S. (1994). Structural basis for the binding of proline-rich peptides to SH3 domains. Cell *76*, 933–945.

Zahner, J.E., Harkins, H., and Pringle, J.R. (1996). Genetic analysis of the bipolar pattern of bud site selection in the yeast *Saccharomyces cerevisiae*. Mol. Cell. Biol. *16*, 1857–1870.